IFT - UNESP
INSTITUTO DE FÍSICA TEÓRICA

DISSERTAÇÃO DE MESTRADO IFT-D.010/2025

Field Theory for Quantum Thermalization and Statistics of the Spectral Form Factor

Francisco José Divi

Orientador

Prof. Dario Rosa

Novembro de 2025

Divi, Francisco José
D618f Field theory for quantum thermalization and statistics of the spectral form factor / Francisco José Divi. – São Paulo, 2025
61 f: il. color.

Dissertação (mestrado) – Universidade Estadual Paulista (Unesp), Instituto de Física Teórica (IFT), São Paulo
Orientador: Dario Rosa

1. Matéria condensada. 2. Caos quântico. 3. Matrizes randômicas
I. Título

Sistema de geração automática de fichas catalográficas da Unesp. Biblioteca do Instituto de Física Teórica (IFT), São Paulo. Dados fornecidos pelo autor(a).

FIELD THEORY FOR QUANTUM THERMALIZATION AND STATISTICS OF THE SPECTRAL FORM FACTOR

Dissertação de Mestrado apresentada ao Instituto de Física Teórica do Câmpus de São Paulo, da Universidade Estadual Paulista "Júlio de Mesquita Filho", como parte dos requisitos para obtenção do título Mestre em Ciências, área: Física.

Comissão Examinadora:

Prof. Dr. DARIO ROSA(Orientador)
Instituto de Física Teórica/UNESP

Prof. Dr. TOBIAS MICKLITZ
Centro Brasileiro de Pesquisas Físicas/CBPF

Prof. Dr. EDUARDO MIRANDA
Universidade Estadual de Campinas/UNICAMP

Conceito: Aprovado

São Paulo, 19 de novembro de 2025.

Agradecimentos

I would like to thank my collaborators: Alexander Altland, Dario Rosa, Maedeh Rezaei, Silvia Pappalardi and Tobias Micklitz. I have learned a great deal from each of them.

Special thanks go to Dario, who accompanied me throughout my Master's and with whom I greatly enjoyed many stimulating discussions, and to Tobias, from whom I have learned so much through numerous projects and countless discussions.

I would like to thank the Perimeter/ICTP-SAIFR/IFT-UNESP fellowship program supported by FAPESP Project No. 2021/14335-0 and CAPES for financial support. Research at the Perimeter Institute is supported in part by the Government of Canada through the Department of Innovation, Science and Economic Development and by the Province of Ontario through the Ministry of Colleges and Universities.

Resumo

Compreender a termalização em sistemas quânticos a partir de uma perspectiva universal é um desafio fundamental, de grande interesse em caos quântico, holografia e sistemas desordenados. Um ponto crucial nesse contexto é o surgimento da universalidade de matrizes aleatórias em tempos tardios, normalmente diagnosticada por meio do fator de forma espectral (SFF).

Para entender o surgimento do comportamento de matriz aleatória em tempos tardios, discutimos o Quantum Sun Model e derivamos a teoria de campo correspondente. A teoria é semiclassicamente exata, permitindo uma solução completa em seu regime ergódico. O sistema exibe um conjunto de modos massivos que surgem da interferência entre graus de liberdade retardados e avançados. Além disso, discutimos o mecanismo que garante o surgimento de um grau de liberdade sem massa, assegurando o comportamento universal de matriz aleatória em tempos tardios.

Também estudamos as estatísticas do fator de forma espectral na teoria de matrizes aleatórias. Em ordem dominante, essas estatísticas são gaussianas, mas existem correções subdominantes intimamente relacionadas à exatidão semiclassica. Essas correções não gaussianas podem ser obtidas por meio de um cálculo semiclassico, incorporando um conjunto de novos pontos de sela que generalizam as Standard e de Andreev–Altshuler no modelo sigma de Efetov.

Esta tese baseia-se nos resultados da Refs. [1, 2].

Palavras Chaves: Termalização quântica; Fator de forma espectral; Exatidão semiclassica; Caos quântico; Teoria de matrizes aleatórias.

Áreas do conhecimento: Física; Matéria condensada; Sistemas quânticos desordenados.

Abstract

Understanding thermalization in quantum systems from a universal perspective is a key challenge, of central interest in quantum chaos, holography, and disordered systems. A key insight in this context is the emergence of random matrix universality at late times, typically diagnosed through the spectral form factor (SFF).

To understand the emergence of late-time random matrix behavior, we discuss the Quantum Sun Model and derive the corresponding field theory. The theory is semiclassically exact, allowing for a complete solution in its ergodic regime. The system exhibits a set of massive modes arising from interference between retarded and advanced degrees of freedom. We further discuss the mechanism that ensures the emergence of a massless degree of freedom, guaranteeing universal random-matrix behavior at late times.

We also study the statistics of the spectral form factor in random matrix theory. To leading order, these statistics are Gaussian, but there exist subleading corrections intimately related to semiclassical exactness. These non-Gaussian corrections can be obtained by a semiclassical calculation by incorporating a set of new saddles that generalize the Standard and Andreev-Altshuler saddles in Efetov's Sigma model.

This thesis is based on results from Refs. [1, 2].

Keywords: Quantum thermalization; Spectral form Factor; Semiclassical exactness; Quantum chaos; Random matrix theory.

Subject Areas: Physics; Condensed matter; Quantum disordered systems.

Índice

Capítulo 1

Introduction

One of the cornerstones of modern physics is the notion of universality. We have come to understand why systems with vastly different microscopic descriptions can display identical macroscopic behavior, which is often determined exclusively by their symmetries. The renormalization group (RG) is the language through which we have been able to precisely connect symmetries and the flow towards emergent universal behavior [3]. This fruitful perspective lies at the center of the Landau paradigm and effective field theory approaches, which underpin many of our most successful theoretical frameworks.

In recent years, similar ideas have begun to illuminate the structure of quantum chaos and thermalization in isolated many-body systems [4, 5, 6]. Perhaps, one of the oldest (but still modern) questions in quantum many-body systems is: How is unitarity compatible with thermalization?

A more contemporary and refined version of this question is: How does the finite structure of the Hilbert space manifest in late-time correlation functions? [7, 8] This sharper formulation has led to many recent and exciting developments in the study of quantum chaos and holography. In fact, thanks to the holographic duality, this question is intimately related to a version of the black hole information problem, and understanding its answer is related to understanding the fine-grained structure of black hole microstates [9, 10, 11, 12].

Perhaps the most adequate framing of this question for this thesis is: How can we describe quantum ergodic systems from a universal perspective? This is not merely a rich conceptual question; understanding ergodicity and ergodicity breaking is a central question in quantum disordered systems.

In this thesis, we will explore and present some partial answers to these questions from the lens of disordered systems and random matrix-like theories. We will begin by presenting the notion of random matrix universality. Roughly speaking, ergodic systems at late times explore their phase space/Hilbert space uniformly and, consequently, exhibit behavior reminiscent of random matrices [13]. In Chapter 2 we will make this (extremely) vague idea precise, through the notion of causal symmetry breaking and Efetov's Sigma model, an effective field theory for the late-time physics of ergodic systems [5, 13, 14]. This will require presenting and formulating Efetov's supersymmetric approach (Sec. 2.3), suitable for semiclassical, yet non-perturbative calculations in the Hilbert space dimension.

While Efetov's supersymmetric method is extremely powerful, obtaining certain observables can become technically challenging, and the extent of the calculations can sometimes obscure key conceptual points. For this reason, we will also discuss an alternative formulation based on the Keldysh formalism in Sec. 2.4. We will present a modern version of this approach, based on Ref. [15], which is particularly well suited for studying Floquet brickwall systems. Furthermore, we will show that this framework naturally facilitates the computation of various types of correlation functions and their statistics. These aspects, along with their corresponding non-perturbative results, will be explored in Chapters 3 and 4.

Finally, in Chapter 5, we will present and study a modified random matrix–like theory, originally developed to model avalanche instabilities in many-body localized (MBL) systems [4, 6, 16, 17, 18, 19]. We will discuss the various regimes of this model and provide a full solution in the weakly coupled ergodic regime. This will allow us to present a natural-language description of the "flow" or relaxation towards the late-time universal behavior. Our goal is to present a simple picture of quantum effects in thermalization, leaving a more in-depth study of non-perturbative effects in the non-ergodic limit for future work.

Capítulo 2

Effective Theory for Quantum Chaos

The goal of this chapter is to present a quantitative understanding of the late-time behavior of ergodic systems through the lens of quantum chaos and random matrix universality. First, we will refine the questions of interest by introducing one of the central observables in quantum chaos: the spectral form factor (SFF). We will discuss its relevance and review two powerful formalisms that can be employed to compute and, more importantly, to understand it. These formalisms are Efetov's supersymmetric method [14, 13] and the Keldysh formalism [3, 15]. As we will see, they provide a natural framework for formulating and understanding effective theories of quantum correlations in ergodic systems.

Let us spoil the answer: in ergodic systems, spectral correlations are described by a low-energy effective theory exhibiting causal symmetry breaking [5]. As a result, ergodic systems present a set of light (Goldstone) modes which yield correlations in a certain random-matrix universality class. In the following sections, we will unpack this statement and make it more precise.

2.1 Spectral Form Factor

One of the things that we would like to understand is how a finite level spacing, that is, a finite Hilbert space dimension D, can be compatible with thermalization. In other words, we aim for an effective theory of quantum thermalization that has a universal manifestation of the finiteness of D in its late-time physics.

This is still somewhat imprecise, and we need to clarify three specific points. First, what do we mean by low-energy and late-time physics? Here, we are talking about energy scales of order and smaller than the many-body mean level spacing

$$\Delta = \frac{1}{\rho(E)} = O\left(\frac{1}{D}\right) \tag{2.1}$$

where $\rho(E) = \sum_{\mu} \delta(E - \epsilon_{\mu})$ is the density of states. This energy scale has an associated time scale, given by the Heisenberg time

$$t_{\mathrm{H}} = \frac{2\pi}{\Delta} = O(D). \tag{2.2}$$

Second, and thinking from a quantum field theory perspective, how can we extract universal behavior, given that we have a fixed energy scale? A related and perhaps more worrisome issue is that, for a given Hamiltonian realization, there is no guarantee that sample-dependent details are washed out at this fixed scale. This is a subtle matter, closely tied to the very nature of the questions we are asking. A partial answer is that, in order to extract universal behavior, some form of averaging is required [5]. For instance, in a physical system, such averaging may correspond to a smearing of energy levels, while in an ensemble of random Hamiltonian realizations, it may correspond to a disorder average. This is a very subtle point, which we will come back to later.

Third, how can we probe thermalization in a way that is sensitive to finite D effects? We can address these in two ways: from an energy or time perspective.

From a spectral point of view, we should examine how the density of states $\rho(E)$ varies within energy windows of order Δ. While for larger energy scales we expect $\rho(E)$ to be a smooth function of E, at least in the large D limit, the discreteness of the spectrum itself suggests interesting behavior for energy windows of order Δ. Consequently, a natural quantity to consider is the two-level correlation function $\rho(\epsilon)\rho(\epsilon')$. Once again, to extract universal behavior, we are going to need some kind of smearing or averaging, so the interesting observable to look at is

$$R_2(\omega; E) = \left\langle \rho(E+\frac{\omega}{2})\rho(E-\frac{\omega}{2}) \right\rangle - \langle \rho(E) \rangle^2 \tag{2.3}$$

Most of the time, the dependence in E will be uninteresting, so we will set $E = 0$ (center of the spectrum) and work in the energy scale $\omega \sim \frac{1}{D}$.

What happens from the temporal point of view? In this case, the key observable is the time evolution operator and, particularly convenient, its trace. Thus, we could consider the analytically continued partition function

$$Z(t) = \mathrm{Tr}\, e^{-iHt} = \sum_{\mu} e^{-i\epsilon_\mu t}. \tag{2.4}$$

The partition function starts at $Z(0) = D$ and, due to the phase cancellations, it will rapidly start decaying. However, precisely due to the finite structure of the

Hilbert space, Z will not go straight to zero for late times, but rather will remain oscillating around zero.

These fluctuations are the kind of diagnostic of quantum thermalization that we are looking for. They are an intrinsically quantum effect that survives after the system has thermalized. To capture them, it is natural to consider

$$\mathrm{SFF}(t) = |Z(t)|^2 = |\operatorname{Tr} e^{-iHt}|^2, \tag{2.5}$$

called the spectral form factor (SFF).

Note that, while for short times $\mathrm{SFF}(0) = D^2$ and decays rapidly, for late times, its time average is

$$\lim_{T\to\infty} \frac{1}{T} \int_0^T dt\, \mathrm{SFF}(t) = \lim_{T\to\infty} \frac{1}{T} \int_0^T dt \sum_{\mu,\nu} e^{i(\epsilon_\mu - \epsilon_\nu)t} = D \tag{2.6}$$

In fact, we expect this result to hold for $T \gg t_{\mathrm{H}}$.These are the aforementioned late-time fluctuations, revealing the intrinsically quantum nature of the system. This emergence of universal behavior and its accessibility to computations has made the SFF one of the central objects of study in Quantum Chaos [13, 8].

Note that both Eq. (2.3) and Eq. (2.5) are related. To see this connection, consider the Fourier transform of $Z(t)$, the resolvent,

$$G(\epsilon) = \operatorname{Tr}\left(\frac{1}{\epsilon - H}\right). \tag{2.7}$$

Note that G is only well defined for complex ϵ outside of the spectrum of H. Thus, in the large D limit or if we consider any kind of ensemble average, we will encounter issues in defining it on the real axis.

A natural solution to this is adding an infinitesimal imaginary part $G_\pm(\epsilon) = G(\epsilon \pm i\delta)$ with $\delta > 0$. We can understand this infinitesimal part as fixing the causality of the resolvent. For instance, we have

$$\int \frac{d\epsilon}{2\pi} G_+(\epsilon)\, e^{-i\epsilon t} = -i\,\theta(t)\; \operatorname{Tr} e^{-iHt} = -i\theta(t)\, Z(t) \tag{2.8}$$

because we can only close the contour in the lower half-plane. Thus, G_+ corresponds to a retarded Green's function.

This $\delta > 0$ is an auxiliary infinitesimal quantity that we want to take to zero towards the end of the calculation. However, as a result of the anticipated causal-symmetry breaking, this infinitesimal δ-difference will become magnified into a finite branch cut. A short calculation shows that this discontinuity in $\bar{G}(\epsilon)$ is related to the density of states via

$$\text{Im } \bar{G}_{\pm}(\epsilon) = \pm \frac{\bar{\rho}(\epsilon)}{\pi}. \tag{2.9}$$

where the bars denote an ensemble average or smearing in some energy window. We will see an explicit example of this in the next section. This is a key conceptual point, which will expand in Sec. 2.3.4.

Lastly, the connection between these two approaches can be explicitly made by noticing that for $t > 0$, we have

$$\text{SFF}(t) = \int dE_1 dE_2 \, \langle \rho(E_1)\rho(E_2) \rangle \, e^{i(E_1 - E_2)t} = \int dE d\omega \; R_2(\omega, E) e^{-i\omega t}, \tag{2.10}$$

which allows us to recover the SFF after working in frequency space.

2.2 Random Matrix Universality

We have the first piece of the puzzle: the SFF and R_2 are observables that capture interesting quantum correlations in the time/energy scale of interest. Now, we would like to quantify what they look like for ergodic systems.

In Chapter 1, we hinted at part of the answer. We mentioned that we can expect ergodic systems to behave, in some sense, like random matrices. But in which sense?

A partial answer to this question was provided by Wigner [20]. Wigner's insight was that, at late times, strongly interacting many-body Hamiltonians look so complicated that they behave like random matrices. For instance, consider the time evolution

$$U = e^{-iHt}. \tag{2.11}$$

In a given physical basis (think, for example, working in the computational basis of a local spin chain) H is very sparse, with only a few non-vanishing entries. As we start increasing t, higher powers of H^k dominate the Taylor expansion of the exponential, making U look more and more "random". Of course, you can always evolve back or write your problem in the energy basis, revealing the non-randomness of H, but in a given fixed, "reasonable" basis, the many-body correlations are so involved that you cannot extract them with any simple protocol.

This is entropy at play.

There is a small caveat: we should always keep symmetries in mind. If a Hamiltonian, for example, preserves particle number, then at late times it can only look like a "random matrix" within sectors of fixed particle number.

Now, how can we profit from this intuition? One way is to look at the statistics of energy levels. Up to symmetries, and on the appropriate energy scale, the energy statistics of ergodic many-body systems should resemble those of a random matrix. This has been tested across a wide range of systems [13]. In fact, nowadays we use energy statistics as a diagnostic of ergodicity and ergodicity-breaking [4].

With this in mind, a natural step toward understanding quantum effects in thermalization is to study random matrices, which we will do next.

2.2.1 Gaussian Unitary Ensemble

One of the simplest random matrix theories that we can consider is matrix models with $U(D)$ symmetry. The idea is to consider an ensemble of hermitian Hamiltonians of size $D \times D$, sampled from a probability distribution $P(H)$ with the symmetry

$$P(H) = P(UHU^{-1}) \tag{2.12}$$

for any unitary $U \in U(D)$. Note that $P(H)$ can only be a function of the moments $\mathrm{tr}(H^n)$.

If we additionally require independence of the entries $P(H) = \prod_{i \leq j} p_{ij}(H_{ij})$, we arrive at the Gaussian Unitary Ensemble (GUE). In this case, the Hamiltonian entries are sampled from a zero-mean Gaussian with variance[1]

$$\left\langle |H_{\alpha\beta}|^2 \right\rangle = \frac{\lambda^2}{D} \tag{2.13}$$

where taking $\lambda = O(1)$, i.e. not scaling with D, ensures a spectrum with finite support in the large D limit. To construct a low-energy field theory for random matrix models with $U(D)$ symmetry, we do not need to work in the GUE, but it will simplify the derivation [5].

One of the remarkable properties of the GUE is its non-trivial, yet simple, density of states. We can evaluate it as follows. Consider the resolvent, Eq. (2.7), and its formal Taylor expansion in powers of H. In the large D limit, we can evaluate the average resolvent by summing over non-crossing Wick contractions

[1]For the diagonal entries, which are real, we actually require $\langle H_{\alpha\alpha}^2 \rangle = \frac{\lambda^2}{2D}$

[21]. The corresponding combinatorics correspond to Catalan's numbers, which can be easily summed to find G. One finds an answer with a finite branch-cut, $G_+ - G_-$, which gives the semicircle density of states

$$\bar{\rho}(\epsilon) = \theta(2\lambda - |\epsilon|)\frac{\sqrt{(2\lambda)^2 - \epsilon^2}}{2\pi\lambda^2}. \tag{2.14}$$

This is a celebrated result, originally due to Dyson [22]. We observe that states accumulate near the center of the band at $\epsilon = 0$ and, on average, are supported in the energy window $\epsilon \in (-2\lambda, 2\lambda)$.

We may wonder whether the same trick works to determine the two-point correlation R_2, Eq. (2.3). However, the analysis becomes more involved and is not particularly suitable for studying non-perturbative effects in D. As a result, many methods have been developed that enable not only simpler but also conceptually richer approaches to understanding quantum thermalization through R_2 and the SFF. These will be the object of Sections 2.3 and 2.4.

2.2.2 Circular Unitary Ensemble

There is an alternative way to construct an ensemble of systems with $U(D)$ symmetry. Instead of sampling Hamiltonians, we could have sampled the time evolution operator. This change of perspective requires discretizing time, making the dynamics those of a "random circuit" or Floquet system

$$U_t = U^t \quad \text{with} \quad U \sim \text{uniform} \quad t \in \mathbb{N}\,, \tag{2.15}$$

where U is being sampled uniformly from the unitary group [13].

As a result, the average density of states, now understood as the phases of the eigenvalues of U, becomes uniformly distributed in the unit circle: $\overline{\rho}(\epsilon) = \frac{D}{2\pi}$. Thus, the Heisenberg time is $t_{\mathrm{H}} = 2\pi\bar{\rho} = D$. This is a "circular" density of states that simplifies the issue of a non-constant density of states in the GUE, which is quite convenient in some scenarios, see e.g., Sec. 2.4.

In some sense, the advantages of discretizing time are analogous to those of discretizing space in QFT, providing a natural UV cutoff that simplifies many of the intrinsic difficulties in defining a QFT. However, it also comes with the inconvenience of working with discrete rather than continuous variables. For the purposes of this thesis, the difference between the two ensembles will be largely irrelevant, and we will freely move back and forth between them.

2.3 Efetov's sigma model for RMT

In this section, we present some of the basics of Efetov's supersymmetric approach [13, 14]. We will employ a bottom-up approach, starting from the microscopic ("UV") theory, switching to a more convenient representation in terms of the collective variables, and arriving at the low-energy ("IR") effective theory: Efetov's sigma model.

To perform such a derivation, we will write a generating function for Eq. (2.3) and express it as a matrix integral involving both commuting and anticommuting variables. The advantage of this is that it allows the disorder average to be taken at a very early stage of the calculation. The resulting theory inherits several symmetries, allowing us to describe the problem in terms of collective modes that efficiently capture the late-time behavior of observables.

2.3.1 Derivation of the sigma model

To write a generating function for Eq. (2.3), we start from a simple observation

$$\frac{\partial}{\partial\alpha}\frac{\det(X+\alpha)}{\det(X)}\bigg|_{\alpha=0} = \mathrm{tr}\left(X^{-1}\right) \tag{2.16}$$

As a result, we introduce the following generating function

$$\mathcal{Z}(\vec{z}) = \frac{\det(z_1 - H)\det(z_2 - H)}{\det(z_3 - H)\det(z_4 - H)}. \tag{2.17}$$

where $\vec{z} = (z_1, z_2, z_3, z_4)$. This allows us to obtain G by taking derivatives with respect to z_i, then canceling the remaining determinants by setting, for example, $z_1 = z_3$ and $z_2 = z_4$.

But here we have to be careful. Recall that G is not well defined on the real axis, so we need to fix the causality of the correlation function by adding infinitesimal imaginary parts. To obtain R_2, containing two densities of states, we need to pick two advanced and two retarded resolvents. One possibility is

$$\vec{z} = (z_1^+, z_2^-, z_3^+, z_4^-) \tag{2.18}$$

where $z_i^{\pm} = z_i \pm i\delta$. Thus, we can obtain [13]

$$\langle \rho(\epsilon)\rho(\epsilon')\rangle_H = \frac{1}{\pi^2}\mathrm{Re}\frac{\partial}{\partial z_1}\frac{\partial}{\partial z_2}\langle \mathcal{Z}\rangle_H(\epsilon,\epsilon',\epsilon,\epsilon') \tag{2.19}$$

Now, the big difficulty in this calculation is how to compute the disorder average. Previously, we formally expanded in powers of H and considered Wick contractions, but that is not convenient anymore. The idea of Efetov's approach is to represent determinants as integrals over bosonic or fermionic variables ("ghosts") and perform the disorder average immediately after.

More precisely, introduce the fermionic (bosonic) variables $\chi_\alpha^{\pm}$ ($S_\alpha^{\pm}$), where $\pm$ distinguishes between 1 and 2 (3 and 4), respectively, and $\alpha = 1,\ldots,D$. We then group all the variables into a single $4D$-dimensional supervector [14]

$$\psi = \begin{pmatrix} \chi \\ S \end{pmatrix} \tag{2.20}$$

and write

$$\mathcal{Z} = \int D\psi\, e^{i\bar{\psi}(z-H)\psi}, \tag{2.21}$$

where we have introduced $\bar{\psi} = (\bar{\chi}^+,\bar{\chi}^-,\bar{S}^+,-\bar{S}^-)$, where the minus sign is to ensure convergence in the bosonic sector, in consonance with our previous selection, Eq. (2.18). Thus, convergence requires $\mathrm{Im}(z_3 > 0)$ and $\mathrm{Im}(z_4 < 0)$, fixing the causality in the bosonic sector. As a result, integration over S gives the determinants in the denominator, while integration over χ gives the ones in the numerator.

Now, we are ready to take the ensemble average by performing the Gaussian integral over H. We arrive at

$$\langle \mathcal{Z}\rangle_H = \int D\psi\, e^{i\bar{\psi}z\psi - \frac{\lambda^2}{2D}\sum_{\alpha,\beta,r,s}\bar{\psi}_\alpha^s\psi_\beta^s\bar{\psi}_\beta^r\psi_\alpha^r}, \tag{2.22}$$

where $r,s = 1,\ldots,4$. As a result, we have traded the ensemble average for an effective interaction between bosonic and fermionic degrees of freedom. Importantly, the $U(D)$ symmetry remains manifest:

$$\psi \to \mathbb{1}_4 \otimes U\,\psi \qquad \bar{\psi} \to \bar{\psi}\,1_4 \otimes U^{\dagger}. \tag{2.23}$$

In fact, this symmetry has a very important consequence: it greatly constrains the dependence on the ψ-variables. This symmetry guarantees that the only dependence will come from the collective variables

$$Q^{ss'} = \frac{\lambda}{D}\sum_{\alpha}\psi^{s}_{\alpha}\bar{\psi}^{s'}_{\alpha} \tag{2.24}$$

Let us stress that this observation is independent of the fact that our theory is Gaussianly distributed: it is inherited from the $U(D)$ symmetry. This means that in more general theories, we will still be able to write an effective theory in terms of collective degrees of freedom Q. It is just going to be more involved. In such cases, the disorder average can be made by a color-flavor transformation [5].

To fully leverage this important observation, we can introduce a Lagrange multiplier to decouple the interaction. In the GUE case, this is equivalent to performing a Hubbard-Stratonich transformation by means of the identity

$$e^{-\frac{\lambda^2}{2D}\sum_{\alpha,\beta,r,s}\bar{\psi}^{s}_{\alpha}\psi^{s}_{\beta}\bar{\psi}^{r}_{\beta}\psi^{r}_{\alpha}} = \int DQ\exp\left(\frac{D}{2}\mathrm{Str}(Q^2) - \lambda\bar{\psi}Q\psi\right), \tag{2.25}$$

which can be easily obtained from $\int DQ\; e^{\frac{D}{2}\mathrm{Str}\;Q^2} = 1$, where $\mathrm{Str}A = \mathrm{Tr}\,A_{bb} - \mathrm{Tr}\,A_{ff}$ [14, 13].

This leaves us with a quadratic action over the superfields ψ, which can be immediately performed to yield

$$\langle\mathcal{Z}\rangle_H = \int DQ\exp\left(\frac{D}{2}\mathrm{Str}Q^2 - D\,\mathrm{Str}\log(z + i\lambda Q)\right). \tag{2.26}$$

Up to this point, we have made no approximation, and everything is exact. Now, we will make use of the large D limit to derive the effective low-energy description.

The prefactor of D in the action invites a saddle approximation. Fixing the units by taking $\lambda = 2$ and working close to the center of the spectrum $z \sim \frac{1}{D}$, the saddle point equation reduces to

$$Q^2 = 1. \tag{2.27}$$

The important observation is that everything that does not satisfy this constraint will correspond to very massive modes, strongly suppressed in $\frac{1}{D}$. Therefore, we will restrict ourselves to the space of Q supermatrices satisfying the non-linear constraint Eq. (2.27). In other words, the low-energy physics corresponds to a non-linear sigma model satisfying such a constraint.

It is important to note that this discussion is intimately related to the symmetries of our problem. First, because the collective variables Q is ensured by $U(D)$, as discussed above, and, second, because the non-linear constraint is associated with the "kinematics" (Hubbard–Stratonovich/color-flavor transformation). In this precise sense, the non-linear sigma model provides the universal language to discuss $U(D)$ matrix theories.

Finally, we expand the log to leading order, since "higher-loop" corrections are suppressed in $\frac{1}{D}$ for $z \sim \frac{1}{D}$, arriving at Efetov's non-linear sigma model [14]

$$\mathcal{Z}(\vec{z}) = \int_{Q^2=1} dQ\, e^{iD\,\mathrm{Str}(zQ)}. \tag{2.28}$$

2.3.2 Deriving the Two-level Correlation Function

Now, we want to explicitly compute this matrix integral to obtain the 2-point correlation function via Eq. (2.19) and from there the SFF. Towards this direction, a natural first step is to parametrize the target space, Eq. (2.27).

Here, there is an important caveat. There is a priori no guarantee that all Q configurations can be obtained by deforming the contour of integration in Eq. (2.26). In fact, because the bosonic sector is non-compact, we get strong constraints on the structure of saddles and orbits for this sector: convergence requires $\mathrm{Im}(z_3 > 0)$ and $\mathrm{Im}(z_4 < 0)$, fixing the causality in the bosonic sector.

Standard Saddle - Perturbative result

It turns out that there are 2 important sectors that we need to take into account [13]. The first sector is the simplest saddle that we can take with the right causality in the bosonic sector:

$$Q_0 = \Lambda = \sigma^3_{ra} \otimes \mathbb{1}_{bf}. \tag{2.29}$$

That is, we keep the causal structure of Eq. (2.18). This is known as the Standard saddle and, as we will show next, gives the distinctive ramp to the SFF.

Of course, multiple configurations can be obtained from orbits starting from Eq. (2.29):

$$Q = TQ_0T^{-1} \tag{2.30}$$

That is why we talk about a sector. To carry out an explicit calculation, we need to parametrize these orbits. A very natural choice is an exponential parametrization

[5, 13]

$$T = e^{W} \qquad W = \begin{pmatrix} 0 & B \\ \tilde{B} & 0 \end{pmatrix} \qquad B = \begin{pmatrix} z & \chi \\ \eta & w \end{pmatrix} \qquad \tilde{B} = \begin{pmatrix} \bar{z} & \bar{\eta} \\ \bar{\chi} & -\bar{w} \end{pmatrix} \tag{2.31}$$

where z, w are bosonic variables and η, χ are fermionic variables. Other useful parametrizations are the rational and polar/radial parametrizations. The rationale behind this W is that we are removing the part of the fluctuations that commute with the saddle Λ and keeping only the part that anticommutes: $W\Lambda + \Lambda W = 0$. Of course, if we consider a different saddle, we will need to use a different structure for W. To see a more extensive and complete discussion regarding the target manifold and its parametrizations, see [13].

Next, we will expand the action to quadratic order in the "pion" fields B, $\tilde{B}$. Also, let's use the following source

$$z = \frac{1}{2}\Lambda(\omega + \alpha k) \tag{2.32}$$

where $k = \sigma^3_{bf}$. The reason is that it allows us to conveniently compute the SFF as follows [13, 23]

$$R_2(\omega) = \left\langle \rho(\frac{\omega}{2})\rho(-\frac{\omega}{2}) \right\rangle_H = -\frac{1}{(2\pi)^2}\mathrm{Re}\frac{\partial^2}{\partial\alpha^2}\mathcal{Z}(\omega, \alpha = 0) \tag{2.33}$$

Note that $\omega = \omega + i0^+$, according to our choice of causality in Eq. (2.18). With this source, we find

$$\mathcal{Z}_{\mathrm{SS}}(\omega, \alpha) = \int DB\, e^{iD(\alpha + \mathrm{str}((\omega + \alpha k)\tilde{B}B))} \propto -e^{iD\alpha}\frac{\omega^2}{\omega^2 - \alpha^2} \tag{2.34}$$

As a result, the contribution to the two-level correlation function coming from the Standard saddle is

$$R_2^{\mathrm{SS}}(\omega) \propto -\mathrm{Re}\frac{\partial^2}{\partial\alpha^2}Z_{\mathrm{SS}}(\omega, \alpha) = -\frac{1}{\omega^2} + \frac{D^2}{2} \tag{2.35}$$

Fourier transforming for $t > 0$, we get the semiclassical contribution coming from the Standard Saddle

$$\mathrm{SFF}_{\mathrm{SS}}(t) = t \tag{2.36}$$

In other words, and as anticipated, we obtain the ramp. This ramp was obtained by the singular behavior of the 2-point correlation $R_2^{\mathrm{SS}}(\omega) \propto -\frac{1}{\omega^2}$. Thus, we can think of the physical origin of this linear growth as coming from the spectral rigidity associated with the level repulsion.

This obviously cannot be the full result. As discussed below Eq. (2.5), we know that for $t \gg t_{\mathrm{H}}$ the SFF should reach (on average) a plateau value of $\mathrm{SFF}(\infty) = D$. While early-time physics is not accessible to our computation (by its very nature), reproducing the late-time physics is among our main goals. So, what are we missing?

2.3.3 Andreev-Altshuler Saddle - Non-perturbative result

To get the full semiclassical solution, we also need to take into account other saddles. In particular, we are missing a full sector given by fluctuations around the Andreev-Altshuler Saddle (AA) [23]

$$Q_{\mathrm{AA}} = \Lambda k \tag{2.37}$$

where $k = \sigma^3_{bf}$. As we will see next, the corresponding semiclassical contribution will correct our previous contribution to include the plateau.

To compute this new contribution, we could naively think of parameterizing the action in terms of generators that anticommute with the saddle and perform the corresponding expansion. However, there is a nice trick, originally due to Andreev and Altshuler [23], which consists of first performing a global rotation $Q' = T_0^{-1} Q T_0$ such that the saddle is mapped to $Q'_{AA} = T_0^{-1} k \Lambda T_0 = \Lambda$. Since the transformation leaves the action measure invariant, its only effect will be to modify the sources

$$z = \frac{1}{2}(\omega + \alpha k)\Lambda \;\rightarrow\; z' = \frac{1}{2}(\alpha + \omega k)\Lambda \tag{2.38}$$

where we have used that $T_0 \Lambda T_0^{-1} = k\Lambda$ and $T_0 k \Lambda T_0^{-1} = \Lambda$. In other words, it has the exact same form as the Standard saddle but swapping $\alpha \longleftrightarrow \omega$.

It then immediately follows that the AA saddle contributes to the generating function by

$$\mathcal{Z}_{\mathrm{AA}}(\omega, \alpha) = \mathcal{Z}_{\mathrm{SS}}(\alpha, \omega) \propto -e^{iD\omega} \frac{\alpha^2}{\alpha^2 - \omega^2} \tag{2.39}$$

As a result, we get

$$R_2(\omega) = -\mathrm{Re}\frac{1 - e^{iD\omega}}{\omega^2} = -\frac{1 - \cos(D\omega)}{\omega^2} \tag{2.40}$$

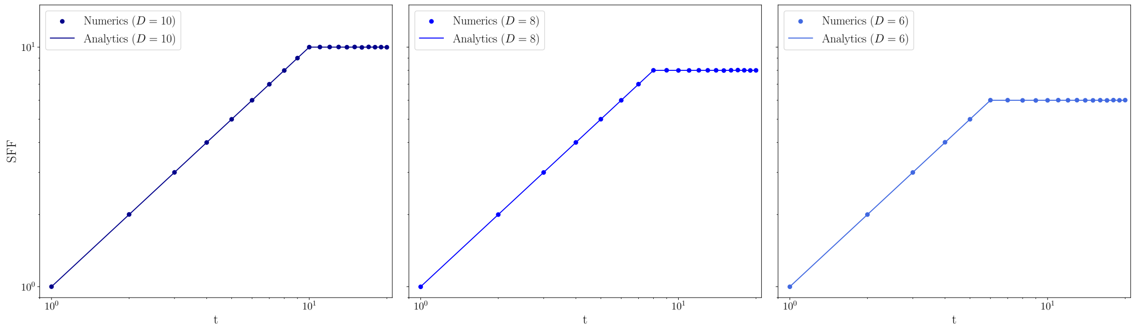

Figura 2.1: Spectral form factor (SFF) computed in the CUE for $D = 10,\ 8,\ 6$ for 10^6 realizations.

Fourier transforming, we obtain the final result

$$\mathrm{SFF}(t) = \begin{cases} t & \text{for } t < D \\ D & \text{for } t > D \end{cases} \tag{2.41}$$

This result is depicted and compared with numerics in Fig. 2.1. We observe an outstanding agreement, even for relatively small system sizes $D < 10$. To understand the origin of this surprising agreement we will explore the role of higher order corrections in Sec. 2.4.

2.3.4 Causal Symmetry Breaking

In this section, we briefly interpret these results following Ref. [5]. As we have highlighted throughout these sections, there are two very important ingredients in our construction: symmetry and causality.

First, we have the $U(D)$ symmetry, which manifests itself in the description in terms of the collective variable Q. As a result, symmetry dictates that the low-energy physics is controlled by a non-linear sigma model, $Q^2 = 1$.

The second ingredient is causality: right from the outset, deciding to probe a quantum-chaotic correlation function, the SFF, forces us to make an (infinitesimal) choice ($G_{\pm}$). What may come as a surprise is that this infinitesimal imaginary part becomes amplified into a finite branch cut, $\mathrm{Im}(G_+ - G_-) \propto \rho \propto D$. This is a symptom of symmetry breaking.

But how can we understand this symmetry breaking from our field theory? If we consider

$$\mathcal{Z} = \int DQ \, \exp\left(\frac{D}{2}\mathrm{Str}Q^2 - D\,\mathrm{Str}\log(z + i\lambda Q)\right), \tag{2.42}$$

we observe the presence of the symmetry $Q \to TQT^{-1}$ with $T \in U(1,1|2)$, weakly broken by the presence of the source z. However, localizing the matrix integral around the standard and AA saddles strongly breaks the symmetry down to $U(1|1) \times U(1|1)$. As a result, the theory presents a Goldstone mode living in $\frac{U(1,1|2)}{U(1|1)\times U(1|1)}$. These are our massless pion fields B[2].

Besides offering a beautiful interpretation of our calculation, the punchline of this argument is that the presence of the massless "singlet" mode B is guaranteed by the symmetry-breaking pattern. This is the universal emergence of ergodicity in the late-time physics. Later on, in Chapter 5, we will discuss a modification of this theory, which will allow us to present a different picture of the emergence of this massless ergodic mode from a set of massive modes, using a diagrammatic language.

2.4 Keldysh Formalism

One of the most striking points from our previous discussion was the precision of the semiclassical calculation. Indeed, simply accounting for the saddles' action and the Gaussian fluctuations around them seems sufficient to accurately describe the SFF (Fig. 2.1). This is a hint of the phenomenon of semiclassical exactness: for certain observables, the semiclassical theory actually gives the exact answer.

We will use this as a partial motivation to present and discuss an alternative, complementary approach: the Keldysh formalism. In contrast to Efetov's method, the Keldysh approach is more naturally formulated in real time, particularly in a discrete-time setting, such as the CUE (Sec. 2.2.2). Semiclassical exactness is only a partial motivation because, as we will shortly see, the Keldysh formalism also proves particularly efficient for treating both SFF statistics and other correlation functions, such as two-point functions (2PFs), out-of-time-order correlators (OTOCs), higher-order OTOCs, and so on, at the perturbative level. This will be the subject of the following chapter.

The method discussed in this section is mostly based on Ref. [15], which pre-

[2] Here, "massless" means that if we turn off the source ($\alpha = 0$), the propagators are, for example, $\langle \bar{B}_{bb} B_{bb} \rangle = \langle \bar{z} z \rangle = \frac{1}{\omega}$, with no self-energy.

sents the Keldysh formalism for Floquet systems (random quantum circuits/brick-wall models).

2.4.1 Deriving the Field Theory

Let us consider the time evolution given by the CUE

$$U_t = U^t \quad \text{with} \quad U \sim \text{uniform} \quad t \in \mathbb{N}\,, \tag{2.43}$$

where U is being sampled uniformly from the unitary group [13].

To write a generating function for the SFF, we start with a simple observation

$$\frac{\partial}{\partial\alpha} \det(1+\alpha X)\bigg|_{\alpha=0} = \operatorname{tr}(X) \tag{2.44}$$

Therefore, we may consider

$$\mathcal{Z}(\theta_+,\theta_-) = \det\left(1 - e^{i\theta_+} U^t\right) \det\left(1 - e^{i\theta_-} U^{\dagger^t}\right). \tag{2.45}$$

as a generating function for the SFF. From it, we can obtain

$$\text{SFF}(t) = \int \frac{d\theta_+ d\theta_-}{(2\pi)^2}\, \mathcal{Z}(\theta_+,\theta_-)\, e^{-i(\theta_+ - \theta_-)}. \tag{2.46}$$

To verify this formula, one formally expands Eq. (2.45) in powers of $e^{i\theta_\pm}$. Note that convergence requires, as usual, adding an infinitesimal imaginary part: $\theta_\pm = \theta_\pm \pm i\delta$, which fixes the causality.

Next, we develop an integral representation of this generating function. Recall that to derive a path integral representation from a Hamiltonian or evolution operator, the main step is to trotterize the time evolution. In the current problem, we can follow this approach employing Grassmann variables, see [15]. However, we will use an arguably cleaner method, which will be easier to generalize to other correlation functions in the following chapter.

First, it will be useful to have the following diagrammatic representation in mind

$$\mathrm{SFF}(t) =$$

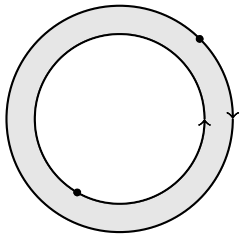

Here, the outer circle denotes a trace over forward time propagation U^t, while the inner circle denotes a trace over backward propagation $U^{\dagger^t}$. Both circles have radius t. The small dot represents the time origin ($n = 1$) and end ($n = t$). The region between the circles is shaded because we expect both circles to "interact" due to the CUE average; see the following discussion.

Accordingly, we want to introduce a causal structure ($s = \pm$) and time structure ($n = 1, \dots, t$). This can be achieved as follows. If the original trace is over some vector space V, we will now consider a larger space $V \otimes V_t$, where $\dim V_t = t$ is the time structure. Next, we introduce $T_\pm$, the hopping operators with periodic boundary conditions in this time space V_t: $T_\pm |n\rangle = |n+1\rangle$ for $n = 1, \dots, t$. Thus, we can write

$$\mathrm{tr}\log\left(1 - X^t\right) = \mathrm{Tr}\log(1 - T_\pm X) \tag{2.47}$$

where now Tr is a trace over $V \otimes V_t$. As a result, we can write

$$\mathcal{Z}(\theta_+, \theta_-) = \mathrm{Det}(1 - e^{i\phi_+} T_- U)\, \mathrm{Det}(1 - e^{i\phi_-} T_+ U^\dagger) \tag{2.48}$$

where $\theta_\pm = t\phi_\pm$.

Next, we represent this determinant as an integral over Grassmann variables $(\psi_n^\pm, \bar\psi_n^\pm)$ and write

$$\mathcal{Z}(\theta_+, \theta_-) = \int d(\bar\psi, \psi)\ \exp\left(\bar\psi\psi - \psi^+ e^{i\phi_+} \mathcal{T}_- U \psi^+ + \psi_- e^{i\phi_-} \mathcal{T}_+ U^\dagger \psi^-\right) \tag{2.49}$$

This is the desired integral representation of the generating function for the SFF.

We still have to deal with the average over the Haar group, which we attack next. In the Keldysh formalism, the most convenient way to perform the average over the CUE is by an identity called color-flavor transformation [13, 15, 24]

$$\int dU\, e^{\bar\phi^+ U \psi^+ + \bar\psi^- U^\dagger \phi^-} = \int dB\, e^{-D\ \mathrm{tr}\log\left(1 + B^\dagger B\right) - \bar\phi^+ B \phi^- + \bar\psi^- B^\dagger \psi^+}, \tag{2.50}$$

where the integral over the right-hand side is over the matrix fields $B = B_{nm}$, with $n,\ m = 1, \dots, t$.

As a result, the color-flavor transformation replaces the average over the unitary group for a matrix integral. At first glance, there is no gain. However, the benefit is two-fold: it simplifies the physical Hilbert space structure and pivots the description of the theory from the "UV" Grassman fields ψ, to the soft modes/coarse-grained variables of the theory. This will facilitate how to approximate the theory to our energy/time scales of interest.

After the color-flavor, we simply integrate out the fermions and find

$$\mathcal{Z}(\theta_+,\theta_-) = \int DB\ \exp\Big(-D\,\mathrm{tr}\log\Big(1+B^\dagger B\Big) + D\,\mathrm{tr}\log\Big(1+B^\dagger B_T\Big)\Big) \tag{2.51}$$

where $B_T = e^{i\phi}\mathcal{T}B = e^{i(\phi_+-\phi_-)}\,T_-BT_+$ or $(B_T)_{nm} = e^{i\phi}B_{n-1,m-1}$.

Since B_T is, up to the phase, just a time displacement of B, it is natural to introduce the discrete derivative

$$dB = B - B_T = (1-e^{i\phi}\mathcal{T})B. \tag{2.52}$$

Note that $d = (1-e^{i\phi}\mathcal{T})B$ is an operator acting on the matrix space B_{nm}. In this language, the generating function for the SFF reads

$$\mathcal{Z} = \int DB\ \exp\left(D\,\mathrm{tr}\log\left(1-\frac{1}{1+B^\dagger B}B^\dagger dB\right)\right) \tag{2.53}$$

Lastly, we recall that we are interested in the late-time physics, where we expect B to depend smoothly on time, so that dB is small compared to B. To parallel our previous discussion (Sec. 2.3), we can write everything in frequency space and note that $d \sim i\omega$. Therefore, to obtain the analogue theory of Efetov's sigma model, Eq. (2.28), we need to expand the log to linear order to arrive at

$$\mathcal{Z}_{\mathrm{IR}} = \int DB\ \exp\left(-D\,\mathrm{tr}\left(\frac{1}{1+B^\dagger B}B^\dagger dB\right)\right). \tag{2.54}$$

2.4.2 Equivalence with Efetov's sigma model

The Keldysh and supersymmetric approaches are equivalent, they simply offer different perspectives, making different features manifest. However, establishing such equivalence is not immediately obvious by just looking at Eq. 2.28 and Eq. 2.54, except perhaps due to the suggestive notation of using B to denote in both models the massless pion field.

To connect with the sigma model, we need to introduce a causal (retarded/advanced) space. This can be achieved by setting [25]

$$Q(B,B^\dagger) = \begin{pmatrix} 1 & B \\ -B^\dagger & 1 \end{pmatrix} \begin{pmatrix} 1 & 0 \\ 0 & -1 \end{pmatrix} \begin{pmatrix} 1 & B \\ -B^\dagger & 1 \end{pmatrix}^{-1} \equiv T\Lambda T^{-1}. \tag{2.55}$$

A short calculation shows that

$$T^{-1} = \begin{pmatrix} 1 & B \\ -B^\dagger & 1 \end{pmatrix}^{-1} = \begin{pmatrix} 1 & -B \\ B^\dagger & 1 \end{pmatrix} \begin{pmatrix} \frac{1}{1+BB^\dagger} & 0 \\ 0 & \frac{1}{1+B^\dagger B} \end{pmatrix} \tag{2.56}$$

Therefore, we can write

$$-D\,\mathrm{tr}\left(\frac{1}{1+B^\dagger B}B^\dagger dB\right) = \frac{D}{2}\,\mathrm{tr}\left(T^{-1}\Lambda dT\right) \tag{2.57}$$

This is nothing but a discrete time version of the non-linear sigma-model [15]. A great advantage of this representation is that it makes the following symmetry explicitly manifest

$$T \to T_0 T \qquad T^{-1} \to T^{-1}T_0, \tag{2.58}$$

where $T_0 \in U(2)$ is time independent. We will repeatedly use this connection between the two formalisms, both when working with higher moments of the SFF in RMT, Sec. 3.2, and when working with the Quantum Sun Model, in Chapter 5.

2.4.3 Computation of the SFF and Semiclassical Exactness

Now, we will employ this generating function to evaluate the SFF and, finally, discuss why the results agree so well with numerics in Fig. 2.1.

Semiclassical Calculation

First, we consider the semiclassical version of Eq. (2.54), that is,

$$\mathcal{Z}_{\mathrm{sc}}(\theta) = \int DB\ \exp\Big(-D\,\mathrm{tr}\Big(B^\dagger dB\Big)\Big). \tag{2.59}$$

We can justify a posteriori this approximation by noting that the semiclassical propagator is $\langle BB^\dagger\rangle \sim \frac{1}{D}$. Therefore, working with the semiclassical theory corresponds to the leading in D contribution.

Now, Eq. (2.59) simply corresponds to a Gaussian integral and can be performed to yield

$$\mathcal{Z}_{\mathrm{sc}}(\theta) = \frac{1}{\det \mathbb{d}} = \exp(-\operatorname{Tr}\log \mathbb{d}), \tag{2.60}$$

where we wrote $\mathbb{d}$ instead of d to emphasize that it is an operator acting on the matrix vector space $V_t \otimes V_t^*$ (and not just V_t) and, correspondingly, the determinant will be over this matrix vector space.

To explicitly evaluate this, recall that this operator acts as follows $\mathbb{d}\,|n_+, n_-\rangle = |n_+, n_-\rangle - e^{i\phi}\,|n_+ - 1, n_- - 1\rangle$ and therefore only acts non-trivially on the center of mass $\bar{n} = \frac{n_+ + n_-}{2}$, leaving the relative coordinate $\Delta n = n_+ - n_-$ invariant. That is: $|\bar{n}, \Delta n\rangle = |\bar{n}, \Delta n\rangle - e^{i\phi}\,|\bar{n} - 1, \Delta n\rangle$. As a result of this time translation symmetry, we find

$$\mathcal{Z}_{\mathrm{sc}}(\theta) = \exp\Big(-t\,\operatorname{tr}\log\Big(1 - e^{i\phi}\mathcal{T}\Big)\Big), \tag{2.61}$$

where the factor of t corresponds to tracing the trivial relative coordinate $\Delta n = n_+ - n_-$. Using the periodic boundary conditions for $\mathcal{T}$, we get

$$\mathcal{Z}_{\mathrm{sc}}(\theta) = \exp\Big(t\,e^{i\theta} + O(e^{i\theta})\Big) = 1 + t\,e^{i\theta} + O(e^{2i\theta}). \tag{2.62}$$

Therefore, the semiclassical generating function yields the ramp

$$\mathrm{SFF}(t) = t. \tag{2.63}$$

In order to obtain the full SFF, we need to incorporate the plateau physics at $t_{\mathrm{H}} = D$. As we have learned, this is a non-perturbative effect that cannot be captured by any finite-order perturbation theory around the standard saddle and requires including the AA-saddle contribution. However, this non-perturbative analysis becomes quite involved within the Keldysh formalism, so we will omit it (see Refs. [26, 15]).

Semiclassical Exactness

Because we worked at the semiclassical level, the computation was straightforward. But what about higher-order corrections? Naively, one might discard them, as they involve additional propagators and hence higher powers of $\frac{1}{D}$. However, for late-time physics, where $t \sim D$, contributions such as $\frac{t}{D}$ which look subleading in D can become of order one. So, what is going on?

Going back to the sigma model, Eq. (2.54), by expanding the geometric series, we observe that there are a plethora of higher-order corrections that should enter in the calculation:

$$\mathcal{Z}(\theta) = \int DB\, e^{-D\,\mathrm{tr}\left(B^\dagger dB\right)} e^{S_{\mathrm{int}}}, \;\; S_{\mathrm{int}} = \sum_{k=1}^{\infty} S^{(2k)} = D \sum_{k=1}^{\infty} (-1)^{k+1}\, \mathrm{tr}\Big((B^\dagger B)^k B^\dagger dB \Big) \tag{2.64}$$

One would expect all these higher-loop contributions to modify the semiclassical result. Yet, one of the astonishing results of Random Matrix Theory is that for the CUE they actually do not contribute. As we illustrate next, there is a systematic cancellation in Eq. (2.64), making the semiclassical result exact. This is the origin of the astounding agreement with numerics, observed in Fig. 2.1.

To establish the semiclassical exactness, we will need to make some important remarks.

First, from the quadratic action in Eq. (2.59), we can identify the propagator

$$\left\langle B_{n_+ n_-} B^\dagger_{m_- m_+} \right\rangle = \Pi_{n,m} = \frac{1}{D}[d^{-1}]_{n,m} = \frac{1}{D}\delta_{\Delta n, \Delta m} k(\bar{n} - \bar{m}) \tag{2.65}$$

and $k(\bar{n}) = \theta(\bar{n}) e^{i\phi \bar{n}}$ for our theory. Note the propagator is simply a heavyside function as a manifestation of causality.

Second, we note the following contraction rules when averaging over the quadratic theory

$$\begin{aligned} D\left\langle \mathrm{tr}(AB)\,\mathrm{tr}\left(CB^\dagger\right)\right\rangle &= \mathrm{tr}(AC) \\ D\left\langle \mathrm{tr}\left(ABCB^\dagger\right)\right\rangle &= \mathrm{tr}(A)\,\mathrm{tr}(C) \end{aligned} \tag{2.66}$$

which can be easily proven by using that Π and Dd are inverses of each other.

Third, we note that contractions between nearest neighbor fields do not contribute. The reason is essentially causality, which enforces $\Pi_{nn} \propto k(0)$, yielding a disconnected diagram which will always cancel. Equivalently, we can consider the same perturbative expansion in the supersymmetric method[3] and this kind of disconnected diagrams are proportional to $\mathrm{Str}(1) = 0$.

With these three observations, we can start by checking the cancellation of the higher loop corrections order by order. The first order is $S^{(4)} = D\ \mathrm{tr}\left(B^\dagger B B^\dagger dB\right)$, which necessarily involves contraction between nearest neighbor fields and hence will not contribute. The first non-trivial order is the two-loop contribution. Using

[3]To make this connection more precise, we should use a rational parametrization instead of an exponential parametrization. This will yield a one-to-one correspondence between diagrams in both theories.

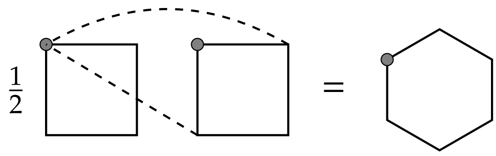

Figura 2.2: Diagrammatic representation of the cancellation at second order. The square represent $S^{(4)} = D\,\mathrm{tr}\big(B^\dagger B B^\dagger dB\big)$ while the hexagon corresponds to $-S^{(6)} = D\,\mathrm{tr}\big(B^\dagger B B^\dagger B B^\dagger dB\big)$. The gray dot corresponds to the discrete derivative d and the dashed lines correspond to possible Wick contractions.

the contraction rules, we find

$$\frac{1}{2}\left\langle S^{(4)} S^{(4)} \right\rangle = \frac{D^2}{2}\left\langle \mathrm{tr}\Big(B^\dagger B B^\dagger dB\Big)^2 \right\rangle = D\left\langle \mathrm{tr}\Big(B^\dagger B B^\dagger B B^\dagger dB\Big) \right\rangle = -\left\langle S^{(6)} \right\rangle \tag{2.67}$$

This cancellation is diagrammatically depicted in Fig. 2.2.

Similarly, one can show the cancellation for the next order

$$\left\langle S^{(8)} \right\rangle + \left\langle S^{(4)} S^{(6)} \right\rangle + \frac{1}{6}\left\langle S^{(4)} S^{(4)} S^{(4)} \right\rangle = 0. \tag{2.68}$$

One can show that this extends to all orders, yielding the anticipated semiclassical exactness of RMT [27]. Again, numerical evidence for this result can be found in Fig. 2.1, where even for relatively small D values we find excellent agreement.

Capítulo 3

Statistics of the Spectral Form Factor

One of the most significant simplifications that certain disordered systems enjoy is "self-averaging". That is, for some problems, certain extensive observables can be treated as non-random variables, i.e. they have trivial statistics. The essential idea is that when correlations are not "large", one can subdivide the full systems into smaller, yet still macroscopic, pieces and treat each of them as an independent realization of the ensemble. Consequently, for self-averaging observables, we can ensemble-average and forget that we are actually dealing with random variables. Conceptually, this is the same principle behind the Central Limit Theorem.

Up until now, our discussion of the SFF has been mostly centered on its expectation value. Yet, even though we are working in the large D limit, we do not have a priori grounds to assume that such quantum correlations are small. In fact, as we will shortly see, the SFF is not self-averaging. Thus, one of the objectives of this chapter will be to understand and describe the statistics of this quantity.

Given that the semiclassical (Gaussian) theory provides such an adequate description of the SFF, a natural guess is that the SFF will have Gaussian statistics. This is almost correct. The effective theory for the SFF, Eq. (2.64), is not Gaussian; it is semiclassically exact. This means that if we want to consider higher moments of the SFF, there will be higher-loop corrections to the Gaussian statistics as a result of the underlying theory not being Gaussian.

To understand and compute the statistics of the SFF, we will first work within the Keldysh formalism to demonstrate the relation between semiclassical theory and Gaussian statistics. This will also allow us to demonstrate semiclassical exactness for the effective theory of SFF^n. However, as we know, this formalism is not very efficient for obtaining and discussing non-perturbative results and, hence, will be inappropriate for discussing corrections to the Gaussian statistics.

Therefore, we will then proceed to a more elaborate calculation using a replicated version of Efetov's sigma model. This will allow us to obtain the non-Gaussian statistics in a semiclassical, non-perturbative calculation by incorporating a set of new saddles that generalize the Standard and Andreev-Altshuler saddles.

This chapter presents some of the results of Refs. [1, 2, 15].

3.1 SFF Statistics: Keldysh formalism

We will start by working in the Keldysh formalism. This will allow us to expose the intimate connection between the semiclassical theory and the Gaussian statistics.

Suppose we want to compute the n-th moment of the SFF: $\langle \mathrm{SFF}^n(t)\rangle$. This means that we will have to consider n replicas of the theory in Eq. (2.45). Thus, consider

$$\mathcal{Z}_n(\theta) = \prod_{s=1}^{n} \det\left(1 - e^{i\theta_+^{(s)}} U^t\right) \det\left(1 - e^{i\theta_-^{(s)}} (U^\dagger)^t\right) \tag{3.1}$$

From where we can extract $\langle \mathrm{SFF}^n(t)\rangle$ by looking at the coefficient of $e^{i\bar{\theta}} = e^{i\sum_s \theta_+^{(s)} - \theta_-^{(s)}}$.

Next, we develop a field theory in terms of the Grassman variables exactly as outlined in Sec. 2.4.1. The only difference is that now the Grassman variables have an additional index corresponding to the replicas: $\psi_n^{\pm s}$. We have

$$\mathcal{Z}_n(\theta) = \int d\psi \exp\left(\bar{\psi}\psi - \psi^+ e^{i\phi_+} T_- U \psi^+ + \psi_- e^{i\phi_-} T_+ U^\dagger \psi^-\right) \tag{3.2}$$

After a color-flavor transformation, we get the same expression as before, Eq. (2.51), with the only subtlety that now the pion fields have also a replica structure $B = B_n^s = B_{n_+ n_-}^{s_+ s_-}$. Working to the lowest in discrete derivatives, we again arrive at

$$\mathcal{Z}_n(\theta) = \int dB \exp\left(-D \operatorname{Tr}\left(\frac{1}{1 + B^\dagger B} B^\dagger dB\right)\right) \tag{3.3}$$

where now Tr involves both time and replica indices.

We can evaluate this semiclassically as before:

$$\mathcal{Z}_n(\theta) = \frac{1}{\det \mathbb{d}} = \exp\left(-t \operatorname{Tr} \log\left(1 - e^{i\hat{\phi}} \mathcal{T}\right)\right) \tag{3.4}$$

where $[e^{i\hat{\phi}}]_{ss',rr'} = \delta_{rs}\delta_{r's'} e^{i(\phi_s^+ - \phi_{s'}^-)}$. Therefore, we get $\mathcal{Z}_n(\theta) = n!\, t^n e^{i\bar{\theta}} + \cdots$ and

$$\langle \mathrm{SFF}^n(t)\rangle = n! t^n = n! \left\langle \mathrm{SFF}\right\rangle^n(t) \tag{3.5}$$

Hence, the semiclassical theory yields Gaussian statistics. This result is compared with numerical simulations in Fig. 3.1.

What about higher-order corrections? Note that the presence of replica structure in the pion fields does not modify the contraction rules, Eq. (5.33)[1]. This means that semiclassical exactness in the original sigma model for SFF, Eq. (2.54), immediately implies semiclassical exactness for the sigma model corresponding to SFF^n, Eq. (3.3).

Does this mean that the SFF has Gaussian statistics? Well, in this section, we only considered the effect of the standard saddle, yet in any semiclassical calculation, one has to consider the potential contribution of all saddles. One could be tempted to conclude that we are only missing the plateau contributions due to the AA saddle. That would be too quick. A more careful analysis shows that the presence of a replica structure allows a new set of saddles to potentially contribute. We will explore these next.

3.2 SFF Statistics: Non-perturbative calculation

To obtain the full statistics of the SFF, we will need to perform a non-perturbative calculation in D, and therefore we will employ Efetov's method. Additionally, to avoid subtleties regarding a non-constant density of states, we will work in the CUE ensemble, whose density of states is constant. For simplicity, we focus on the second moment of the SFF, but the setup for higher moments calculations is similar.

Let us sketch the calculation. First, we will write down a generating function and represent it as a ratio of determinants. Second, we express such ratios as integrals over bosonic and fermionic "ghost" fields. Next, we will average over the Haar ensemble by a color-flavor transformation [24] and rewrite the theory as a generalization of Efetov's sigma model, Eq. (2.28), now involving replica structure. Since we know that the theory is semiclassically exact, we can evaluate it by accounting for each of its saddles and Gaussian fluctuations around them. We will encounter a set of saddles that generalize the Standard and Andreev-Altshuler saddles, and after incorporating their effect, we will be able to compute the non-Gaussian statistics.

[1]The contraction rules still hold as long as we also trace over replica space.

3.2.1 Generating function and non-linear sigma model

The first step is to write a generating function for the second moment of the SFF. Since we are working in the CUE, we start from the following identities

$$\begin{aligned}\mathrm{tr}(U^t) &= \int \frac{d\phi}{2\pi}\, e^{-i\phi t}\, \mathrm{tr}\left(\frac{1}{1-e^{i\phi^+}U}\right),\\ \mathrm{tr}(U^{\dagger t}) &= \int \frac{d\phi}{2\pi}\, e^{i\phi t}\, \mathrm{tr}\left(\frac{1}{1-e^{-i\phi^-}U^\dagger}\right),\end{aligned}$$

with $t \in \mathbb{N}$ the discrete time of evolution and $\phi_s^\pm = \phi_s \pm i0$ slightly shifted into the upper/lower complex plane, fixing the causality.

Therefore, we introduce the generating function

$$\mathcal{Z}(\alpha,\phi) = \left\langle \prod_{i=1,2} \frac{\det\left(1-e^{i(\alpha_i+\phi_i^+)}U^\dagger\right)}{\det\left(1-e^{i\phi_i^+}U^\dagger\right)} \prod_{i=3,4} \frac{\det\left(1-e^{-i(\alpha_i+\phi_i^-)}U\right)}{\det\left(1-e^{-i\phi_i^-}U\right)} \right\rangle_U . \tag{3.6}$$

Indeed, we have

$$\overline{\mathrm{SFF}^2} = \frac{1}{(2\pi)^4}\int d\phi\, \mathcal{F}(\phi)\, e^{-it(\phi_1+\phi_2-\phi_3-\phi_4)} \tag{3.7}$$

$$\mathcal{F}(\phi) = \partial_{\alpha_1}\partial_{\alpha_2}\partial_{\alpha_3}\partial_{\alpha_4}\, \mathcal{Z}(\alpha,\phi)\Big|_{\alpha=0}, \tag{3.8}$$

where $\int d\phi$ denotes integration over all ϕ-variables.

Exactly as in our previous derivation in Sec. 2.3.1, we write the determinants in the numerator and denominator of Eq. (3.6) as integrals involving four complex ('bosonic') and four Grassmann ('fermionic') variables, respectively. Collecting the eight integration variables into the supervector ψ, we obtain

$$\mathcal{Z} = \int_{\mathrm{U}(D)} dU \int d(\bar\psi,\psi)\, e^{\bar\psi(\mathbf{1}_{8D}-E\mathcal{U})\psi}, \tag{3.9}$$

where the integration of bosonic variables is along the imaginary axis, and $\mathbf{1}_{8D}$ is the identity matrix operating in the 8-fold replicated Hilbert space of graded ("bosonic/fermionic"), causal ("retarded/advanced"), and replicated ("1/2") variables. Here, we upgraded the time-evolution operator

$$\mathcal{U} = \begin{pmatrix} U^\dagger & \\ & U \end{pmatrix}_{ra} \otimes \mathbf{1}_2 \otimes \mathbf{1}_{bf}, \tag{3.10}$$

to act on the replicated Hilbert space, where "flavor" indices "ra", "2" and "bf′' denote the subspace of causal, replica and graded indices. Furthermore, we introduced

$$E = \exp(i\Lambda(\phi + \alpha)), \tag{3.11}$$

involving sources and phases organized into matrices

$$\alpha = \mathrm{diag}(\alpha_1, \alpha_2, \alpha_3, \alpha_4) \otimes \pi_f, \tag{3.12}$$
$$\phi = \mathrm{diag}(\phi_1^+, \phi_2^+, \phi_3^-, \phi_4^-) \otimes \mathbf{1}_{bf}, \tag{3.13}$$

where $\pi_f = \frac{1}{2}(1 - \sigma_3^{bf})$ is a projection onto Grassmann components. We also have $\Lambda = \sigma_3^{ra} \otimes \mathbf{1}_2 \otimes \mathbf{1}_{bf}$, following the causal structure of time-evolution Eq. (3.10), as before.

To perform the average over the Haar ensemble, we will again employ a color-flavor transformation [24, 13, 25]. This will exchange the integral over unitaries U, acting on the "color" indices of the Hilbert space, and structureless in flavor space, for an integral over matrices $B,\ \tilde{B}$. These latter, on the other hand, act nontrivially on 'flavor' indices but are structureless in "color" space. Referring for details to the paper, Ref. [1], we notice that the transformation followed by ψ-integration leads to

$$\mathcal{Z} = \int dB\, e^{D\left(\mathrm{Str}\ln\left(1-\tilde{B}B\right) - \mathrm{Str}\ln\left(1-E_+BE_-\tilde{B}\right)\right)}, \tag{3.14}$$

where $E_\pm$ refers to the retarded and advanced sectors of the matrix E.

We have thus arrived at a representation of the generating function in terms of a "flavor" matrix integral involving supermatrices B, $\tilde{B}$. The Haar average has erased all microscopic details. The remaining structures are singlet in Hilbert space, explaining the overall factor D in the exponent of Eq. (3.14).

Before proceeding to the explicit calculation, we can bring Eq. (3.14) to the standard form of a non-linear sigma model, as we did in Sec. 2.4.2 by interpreting B and $\tilde{B}$ as the pion fields in a rational parametrization of [13, 25]

$$Q(B,\tilde{B}) = \begin{pmatrix} 1 & B \\ \tilde{B} & 1 \end{pmatrix} \begin{pmatrix} 1 & 0 \\ 0 & -1 \end{pmatrix} \begin{pmatrix} 1 & B \\ \tilde{B} & 1 \end{pmatrix}^{-1} = T\Lambda T^{-1}, \tag{3.15}$$

fulfilling the non-linear constraint $Q^2 = \mathbf{1}_8$.

Expressed in the variable Q, the matrix integral allows for the compact representation

$$\mathcal{Z} = \int dB\, e^{-D\,\mathrm{Str}\ln\left(1+\frac{1-E}{1+E}Q\Lambda\right)}. \tag{3.16}$$

Anticipating that the correlation function of interest only depends on phase differences and that the Fourier transform fixes phases to values $\phi_1 \simeq \phi_2 \simeq \phi_3 \simeq \phi_4 \sim \mathcal{O}(1/D)$, we can linearize Eq. (3.16) in sources and phases, to obtain

$$\mathcal{Z} = \int dQ\, e^{\frac{iD}{2}\mathrm{Str}((\alpha+\phi)Q)}. \tag{3.17}$$

We note that the linearization $e^{i\phi} - 1 \approx i\phi$ is a matter of convenience, but not essential. In time space, this amounts to an approximation of a discrete-time translation operator by a derivative.

Thus, we have arrived at a two-fold replicated version of Efetov's sigma model, Eq. (2.28). As mentioned above, this matrix integral enjoys "semiclassical exactness", allowing an exact evaluation in terms of "saddle points plus Gaussian fluctuations".

3.2.2 Semiclassical Evaluation

To explicitly evaluate this, we need to understand the structure of saddle points in addition to the standard saddle Λ. We notice that causality fixes the bosonic sector of the saddles to take the form $Q_{\mathrm{bb}} = \sigma_3^{ra} \otimes \mathbf{1}_2$. In the fermionic sector, on the other hand, no such restriction applies, and any of the sixteen matrices $Q_{\mathrm{ff}} = \mathrm{diag}(\pm1, \pm1, \pm1, \pm1)$ provides a legitimate saddle of the sigma-model. In case of the CUE, however, only the traceless matrices, sharing the signature of the standard saddle point, can be accessed[2]. There are thus $\binom{4}{2} = 6$ relevant saddle points for our calculation. They can be parametrized as permutations of the standard saddle Λ and classified by the number of involved transpositions T, as shown in Table 3.1.

A straightforward, if tedious, semiclassical evaluation using the Harish-Chandra-

[2] In the sigma model for the CUE, the rational parametrization in Eq. (3.15) fixes the signature of the saddle, since $\mathrm{tr}\, Q = 0$. In case of the GUE, however, the constraint $Q^2 = \mathbb{1}_8$ is imposed at the semiclassical level, and one needs to consider saddles with different signatures. In this case, fluctuations around saddles with finite trace are suppressed by additional factors $1/D$, and thus subleading [1].

σ	1	2	3	4
I	1	2	3	4
T_{13}	3	2	1	4
T_{14}	4	2	3	1
T_{23}	1	3	2	4
T_{24}	1	4	3	2
$T_{14}T_{23}$	4	3	2	1

Tabela 3.1: Six permutations (σ) giving rise to standard (first entry) and non-standard saddle points (remaining five entries). The last entry corresponds to the Andreev-Altshuler saddle.

Itzykson-Zuber (HCIZ) formula [1, 28, 29], then leads to

$$\mathcal{Z} = \sum_{\sigma} \prod_{i=1,2} \prod_{k=3,4} \frac{(\phi_i - \phi_{\sigma(k)} - \alpha_{\sigma(k)})(\phi_k - \phi_{\sigma(i)} - \alpha_{\sigma(i)})}{(\phi_i - \phi_k)(\phi_{\sigma(i)} - \phi_{\sigma(k)} + \alpha_{\sigma(i)} - \alpha_{\sigma(k)})} e^{\frac{iD}{2}\left(\sum_{i=1,2} - \sum_{i=3,4}\right)(\phi_i - \phi_{\sigma(i)} - \alpha_{\sigma(i)})}, \tag{3.18}$$

and similar results are obtained for the GUE [30].

Next, we compute the contribution of each saddle to the second moment of the spectral form factor. Introducing the compactified notation $\Delta_{ij} = \phi_i - \phi_j$ and performing the four fold derivative, we get

$$\begin{aligned}
\mathcal{F}_I(\phi) &= \left(\frac{D}{2}\right)^4 - \left(\frac{D}{2}\right)^2 \left(\frac{1}{\Delta_{13}^2} + \frac{1}{\Delta_{23}^2} + \frac{1}{\Delta_{14}^2} + \frac{1}{\Delta_{24}^2}\right) + \frac{1}{\Delta_{23}^2\Delta_{14}^2} + \frac{1}{\Delta_{13}^2\Delta_{24}^2}, \\
\mathcal{F}_{T_{13}}(\phi) &= \left(\frac{D^2}{4\Delta_{24}^2} + \frac{iD}{2\Delta_{13}^2}\left(\frac{1}{\Delta_{12}} + \frac{1}{\Delta_{23}} + \frac{1}{\Delta_{43}} + \frac{1}{\Delta_{14}}\right) - \frac{1}{\Delta_{13}^2\Delta_{24}^2} - \frac{1}{\Delta_{12}\Delta_{23}\Delta_{34}\Delta_{41}}\right) e^{iD\Delta_{13}}, \\
\mathcal{F}_{TT}(\phi) &= \frac{\Delta_{12}^2\Delta_{34}^2}{\Delta_{13}^2\Delta_{32}^2\Delta_{24}^2\Delta_{41}^2} e^{iD(\Delta_{13}+\Delta_{24})},
\end{aligned} \tag{3.19}$$

and the other single transposition follow from symmetry.

Finally, we take the Fourier transform. Since $\mathcal{Z}$ only depends on phase differences, one of the ϕ_i will be trivially integrated out. To fix the redundancy related to the poles with identical causal structure ($\phi_1^+ - \phi_2^+$ and $\phi_3^- - \phi_4^-$), we introduce $\phi_s^{\pm} = \phi_s \pm i\delta_s$ and regulate by enforcing $0 < \delta_1 < \delta_2$ and $0 < \delta_3 < \delta_4$ (notice that the result is independent of the chosen order). Extending the remaining integrals over ϕ_i to infinity, and neglecting contributions involving δ-functions in time, we

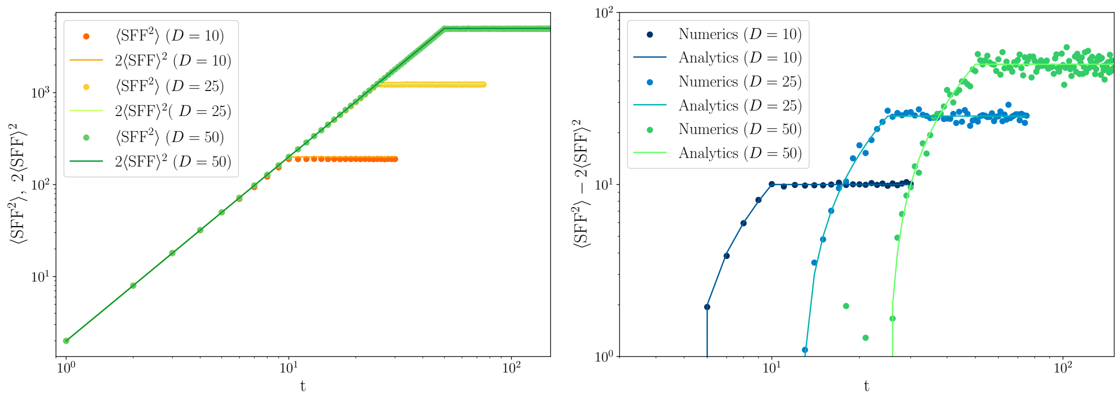

Figura 3.1: Left: Numerical comparison for the second moment $\langle \mathrm{SFF}^2 \rangle$ with $2\langle \mathrm{SFF} \rangle^2$. Discrepancies are suppressed in $\frac{1}{D}$ and are depicted on the right, along with the analytical prediction, Eq. (3.21).

arrive at a disconnected contribution

$$\overline{\mathrm{SFF}^2_{\mathrm{dis}}} = 2 \begin{cases} t^2 & \text{for } t < D \\ D^2 & \text{for } t \geq D \end{cases} = 2\,\overline{\mathrm{SFF}}^2 , \tag{3.20}$$

and connected contribution

$$\overline{\mathrm{SFF}^2_{\mathrm{c}}} = - \begin{cases} 0 & \text{for } 0 < t \leq D/2 \\ 2t - D & \text{for } D/2 < t \leq D\,, \\ D & \text{for } t > D. \end{cases} \tag{3.21}$$

While the disconnected piece, Eq. (3.20), corresponds to the Gaussian statistics, we have found a new contribution, suppressed in $\frac{1}{D}$. One simple check is to consider the long-time average of the second moment

$$\lim_{T\to\infty} \frac{1}{T} \int_0^T dt\, \mathrm{SFF}^2(t) = \lim_{T\to\infty} \frac{1}{T} \int_0^T dt \sum_{\mu,\nu,\alpha,\beta} e^{i(\epsilon_\mu + \epsilon_\nu - \epsilon_\alpha - \epsilon_\beta)t} = 2D^2 - D, \tag{3.22}$$

where the first term corresponds to $(\mu, \nu) = (\alpha, \beta)$ and $(\mu, \nu) = (\beta, \alpha)$ and the last one corresponds to the overcounting $\mu = \nu = \beta = \alpha$.

This result is contrasted with the numerics in Fig. 3.1, observing an excellent agreement. At this point, it is no surprise that the agreement extends even for small D values due to the semiclassical exactness of the non-linear sigma model, Eq. (3.17).

Finally, we comment on the possibility of computing higher moments through the supersymmetric approach. For the k-th moment of the SFF, we need to consider a k-fold replicated theory, which contains a total of $\binom{2k}{k}$ relevant saddles. The same semiclassical evaluation can be carried out, yielding a straightforward generalization of Eq. (3.18). After taking $2k$ α-derivatives, one obtains $\mathcal{F}_k(\phi)$, which can then be Fourier transformed to yield SFF^k. To assess the extent of the difficulty of the calculation for higher orders, we look at the example of $k = 3$. In this case, the generating function becomes a twelve-dimensional integral over bosonic and fermionic fields, and the saddle point structure includes $\binom{6}{3} = 20$ relevant configurations corresponding to traceless sign permutations of the eigenvalue phases. These saddle points generalize those shown in Table 3.1 for $k = 2$. As with $k = 2$, each non-standard saddle contributes to the connected part, and these contributions scale as one order down in $1/D$ compared to the leading Gaussian contribution $\sim 6D^3 z(t)^3$. While the number of relevant saddle point contributions increases combinatorially, the replica formalism systematically organizes their structure, and the semiclassical exactness of the color-flavor transformation ensures that all such terms are captured. This provides a clear and controlled route to studying the full distribution of the SFF beyond the variance.

Capítulo 4

Correlation Functions in Random Matrix Theory

Up to this point, our discussion of quantum thermalization has been primarily centered on the Spectral Form Factor. The main reason is the well-established universality of energy-level statistics, which R_2 and/or the SFF directly prove. However, a complete universal description should also incorporate other observables and correlation functions, such as the two-point function (2PF), four-point function (4PF), and so on. A natural question then arises: to what extent do physically ergodic systems behave like random matrices at late times? This question lies at the heart of the Eigenstate Thermalization Hypothesis (ETH), the full-ETH, and free-probability approaches to quantum chaotic systems [4, 31].

In this chapter, we will complete our discussion of Random Matrix Theory by presenting a formalism for determining correlation functions within the Keldysh framework for Floquet systems. We will illustrate the method for the case of the 2PF, $\mathrm{tr}(\mathcal{A}(t)\mathcal{B})$, emphasizing quantum corrections.

4.1 Two-Point Function

In this section, we develop a framework for constructing generating functions for correlation functions and illustrate how to evaluate them to any desired order in an expansion in $\frac{1}{D}$.

Generating Function

Let us consider the simplest example: the two-point function (2PF)

$$C(t) = \mathrm{tr}(\mathcal{A}(t)\mathcal{B}) = \mathrm{tr}\Big(\mathcal{U}^t\, \mathcal{A}\, \mathcal{U}^{\dagger^t}\, \mathcal{B}\Big) \tag{4.1}$$

in the CUE. Diagrammatically, we can represent this as

$\mathrm{tr}(\mathcal{A}(t)\mathcal{B}) = \mathcal{A}$ 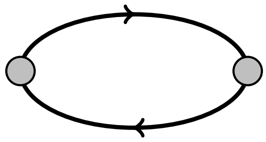 $\mathcal{B}$

In discrete time, this corresponds to the following contour

$$\boxed{0+} \xrightarrow{\mathcal{U}} \boxed{1+} \xrightarrow{\mathcal{U}} \cdots \boxed{t+} \xrightarrow{\mathcal{B}} \boxed{t-} \xrightarrow{\mathcal{U}^\dagger} \boxed{t-1-} \xrightarrow{\mathcal{U}^\dagger} \cdots \boxed{0-} \xrightarrow{\mathcal{A}} \boxed{0+} \tag{4.2}$$

where $\boxed{n\pm}$ correspond to a time index $n = 0, \ldots, t$ and causal contour $\pm$. Importantly, note that this contour of integration is "twisted" by $\mathcal{A}$, $\mathcal{B}$ insertions at the steps $\boxed{0-} \to \boxed{0+}$ and $\boxed{t+} \to \boxed{t-}$, respectively.

We can be reproduce the "effective time evolution" in this contour by considering an "effective evolution operator"

$$\mathcal{U}_{\mathrm{tw}} = e^{i\phi_+} U T_+ \mathcal{P}_+ + e^{-i\phi_-} U^\dagger T_- \mathcal{P}_- + \mathcal{A}\,\Pi_0\,\sigma_{ra}^+ + \mathcal{B}\,\Pi_t\,\sigma_{ra}^- \tag{4.3}$$

where $\Pi_0 = |0\rangle\langle 0|$ is a projector in time indices to $n = 0$ (analogously for Π_t), $\mathcal{P}_\pm = \sigma_{ra}^\pm \sigma_{ra}^\mp$ is a projector to the $\pm$ sector in causal space and $T_\pm$ are clock operators shifting time indices like $T_\pm |n\rangle = |n \pm 1\rangle$. Importantly, note that the hopping operator has open boundary conditions (and not periodic as in the SFF generating function), so that $T_+^{t+1} = 0$ (there is no $|0\rangle\langle t|$ in T_+). Similarly $T_-^{t+1} = 0$.

As a result, we can write the following generating function

$$\mathcal{Z} = \mathrm{Det}(1 - \mathcal{U}_{\mathrm{tw}}) \tag{4.4}$$

where the Tr is over the physical Hilbert space, time, and causal indices. It is not hard to check that $Z(\theta) = -e^{i\theta} C(t) + O(e^{2i\theta})$.

Next, we express the determinant in integral representation

$$\mathcal{Z}(\theta) = \int D\psi \exp\Big(-\bar{\psi}\psi + \bar{\psi}^+ e^{i\phi_+} U T_+ \psi_+ + \bar{\psi}^- e^{-i\phi_-} U^\dagger T_- \psi_- + \bar{\psi}_0^+ \mathcal{A} \psi_0^- + \bar{\psi}_t^- \mathcal{B} \psi_t^+ \Big) \tag{4.5}$$

which, after a color-flavor transformation and integration of the Grassman variables, gives the generating function

$$\begin{aligned}
\mathcal{Z}(\theta) &= \int DB\ \exp\Big(-D\,\mathrm{tr}\log\Big(1 + B^\dagger B\Big) + \mathrm{Tr}\log\Big(1 + B^\dagger B_T + \mathcal{B}\Pi_t B_T - B^\dagger \mathcal{A}\Pi_0\Big)\Big) \\
&= \int DB\ \exp\Big(\mathrm{Tr}\log\Big(1 - \kappa B^\dagger dB + \kappa \mathcal{B}\Pi_t B_T - \kappa B^\dagger \mathcal{A}\Pi_0\Big)\Big)
\end{aligned} \tag{4.6}$$

where $\kappa = \frac{1}{1+B^\dagger B}$. In this way, we have reduced the calculation of the 2PF to the evaluation of this generating function to order $e^{i\theta}$.

Semiclassical Calculation

We start by looking at the lowest order contribution in an expansion in $\frac{1}{D}$. We find

$$\begin{aligned} \mathcal{Z}_{\rm sc}(\theta) &= \int DB\, e^{-D\,\mathrm{tr}\left(B^\dagger d B\right)+\mathrm{tr}(\mathcal{B})\,\mathrm{tr}(\Pi_t B)-\mathrm{tr}\left(B^\dagger \Pi_0\right)\mathrm{tr}(\mathcal{A})} \\ &= -\frac{1}{D}\,\mathrm{tr}(\mathcal{B})\,\mathrm{tr}(\mathcal{A}) k(t) \end{aligned} \tag{4.7}$$

where we have introduced

$$\left\langle B^\dagger_{n_+ n_-} B_{m_- m_+}\right\rangle = \left[d^{-1}\right]_{n,m} = \delta_{\Delta n,\Delta m}\,\theta(\bar{n}-\bar{m})\,k(\bar{n}-\bar{m}) \tag{4.8}$$

with $k(\bar{n}) = e^{i\phi\bar{n}}$ for RMT. Therefore, we find the lowest-order (semiclassical) contribution:

$$\mathrm{tr}(\mathcal{A}(t)\mathcal{B}) = \frac{1}{D}\,\mathrm{tr}(\mathcal{B})\,\mathrm{tr}(\mathcal{A}) + O\left(\frac{1}{D^2}\right). \tag{4.9}$$

If we consider projection operators, $\mathcal{A} = |\mu\rangle\langle\mu|$ and $\mathcal{B} = |\nu\rangle\langle\nu|$, this reduces down to

$$P_{\nu\to\mu}(t) = |\langle\mu|\nu(t)\rangle|^2 \to \frac{1}{D} \tag{4.10}$$

This is the classical statement of thermalization: all states become equally likely at long times, regardless of the initial condition.

Higher loop-corrections

Now, we want to include higher-loop corrections, meaning that we need to perform an expansion in $B, B^\dagger$ in Eq. (4.6). This can become quite involved, so we start by making a simple yet powerful observation.

Note that if we replace $\mathcal{A}\to x\mathcal{A}$, $\mathcal{B}\to y\mathcal{B}$, we see that the $\mathcal{Z}(\theta) = -xy\,e^{i\theta}C(t) + \cdots$, which means that only diagrams with a single insertion of $\mathcal{A}$ and a single insertion of $\mathcal{B}$ can contribute (e.g. we can neglect terms such as $\mathrm{Tr}(\mathcal{A}\cdots\mathcal{A}\cdots)$ which would go like x^2). This will be a significant simplification.

As a matter of fact, there can be only two types of contributions. Thus, we find

$$\mathrm{tr}(\mathcal{A}(t)\mathcal{B}) = f(t)\,\mathrm{tr}(\mathcal{A}\mathcal{B}) + g(t)\,\mathrm{tr}(\mathcal{B})\,\mathrm{tr}(\mathcal{A}) \tag{4.11}$$

where f, g can be computed by a perturbative expansion in $\frac{1}{D}$ and are independent of $\mathcal{A}, \mathcal{B}$.

We can use unitarity (probability conservation) to fix $g(t)$ terms of $f(t)$. Picking $\mathcal{A} = 1$, we find that $Dg(t) + f(t) = 1$. Thus, we must have

$$\operatorname{tr}(\mathcal{A}(t)\mathcal{B}) = f(t)\left(\operatorname{tr}(\mathcal{A}\mathcal{B}) - \frac{1}{D}\operatorname{tr}(\mathcal{A})\operatorname{tr}(\mathcal{B})\right) + \frac{1}{D}\operatorname{tr}(\mathcal{A})\operatorname{tr}(\mathcal{B}) \tag{4.12}$$

If we consider projection operators, $\mathcal{A} = |\mu\rangle\langle\mu|$ and $\mathcal{B} = |\nu\rangle\langle\nu|$, we find

$$P_{\nu\to\mu}(t) = |\langle\mu|\nu(t)\rangle|^2 = f(t)\left(\delta_{\mu\nu} - \frac{1}{D}\right) + \frac{1}{D} \tag{4.13}$$

We find two new contributions. The first one is present only for $\mu = \nu$ and is called the forward-scattering peak. It corresponds to a probability enhancement to remain in the initial condition. This is a result of constructive interference, which, as we will see, survives even for very late times. The other new contribution is isotropic, and it is only there to ensure probability conservation $\sum_\mu |\langle\mu|\nu(t)\rangle|^2 = 1$.

Including Higher-Loop Corrections

To explicitly compute f, we can perform an expansion in powers of $\frac{1}{D}$ by expanding the log in Eq. (4.6) and looking at the coefficient of $\operatorname{tr}(\mathcal{A}\mathcal{B})$. Employing the contraction rules, Eq. (5.33), we will find analogous cancellations to those of Eq. (2.67), making the computation slightly easier.

We find

$$\begin{aligned}\operatorname{tr}(\mathcal{A}\mathcal{B})\left\langle\operatorname{tr}\left(\kappa\Pi_t B_T \kappa B^\dagger \Pi_0\right)\right\rangle_{S_{\text{int}}} &= \int DB\, e^{-D\operatorname{tr}(B^\dagger dB)}\operatorname{tr}\left(B^\dagger B\Pi_t BB^\dagger\Pi_0\right) \\ &= \frac{1}{D^2}\sum_n k(t-n)k(n) = \frac{e^{i\theta}}{D^2}\mathrm{SFF}(t)\end{aligned} \tag{4.14}$$

Diagrammatically, this corresponds to

$$\frac{\mathrm{SFF}(t)}{D^2} =$$

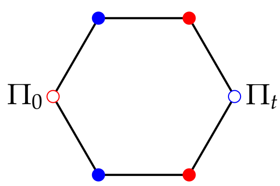

where blue (red) dots represent $B^\dagger$ (B). The final answer is

$$\mathrm{tr}(\mathcal{A}(t)\mathcal{B}) = \frac{\mathrm{SFF(t)}}{D^2}\left(\mathrm{tr}(\mathcal{A}\mathcal{B}) - \frac{1}{D}\,\mathrm{tr}(\mathcal{A})\,\mathrm{tr}(\mathcal{B})\right) + \frac{1}{D}\,\mathrm{tr}(\mathcal{A})\,\mathrm{tr}(\mathcal{B}) \tag{4.15}$$

Which gives

$$P_{\nu\to\mu}(t) = \frac{\mathrm{SFF}(t)}{D^2}\left(\delta_{\mu\nu} - \frac{1}{D}\right) + \frac{1}{D} \tag{4.16}$$

In particular, note that for late times, there is a significant enhancement in the residual probability which (almost) doubles the classical result

$$P_{\nu\to\nu}(\infty) = \frac{2}{D} - \frac{1}{D^3} \tag{4.17}$$

This is a purely quantum effect, as it is manifested by the two-loop correction given by the SFF, Eq. (4.16).

These corrections are depicted and compared with their numerical counterpart in Fig. 4.1 for various matrix dimensions D. The agreement of numerics with Eq. (4.16) is quite remarkable for $D = 50, 100$, but the presence of finite D corrections can be inferred from the discrepancies observed for $D = 10, 25$. This is in stark contrast with the SFF and SFF^2 calculations, which are semiclassically exact.

We can make another interesting observation from Fig. 4.1. For all four systems D, we computed the $P_{\mu\to\mu}(t)$ for 10^6 realizations. Yet, we clearly see that increasing D yields and increasing size make $P_{\mu\to\mu}(t)$ noisier, with larger fluctuations.

To understand this observation and the origin of these fluctuations, we should look at the statistics of $P_{\mu\to\mu}(t)$. If we consider Eq. (4.16), we may estimate

$$\left\langle P^2_{\mu\to\mu}(t)\right\rangle - \left\langle P_{\mu\to\mu}(t)\right\rangle^2 = \frac{\left\langle \mathrm{SFF}^2\right\rangle(t) - \left\langle \mathrm{SFF}\right\rangle(t)^2}{D^4} + \cdots \sim \frac{\left\langle \mathrm{SFF}(t)\right\rangle^2}{D^4} \tag{4.18}$$

up to $\frac{1}{D}$ corrections because of the Gaussian statistics. This means that

$$\frac{\left\langle P^2_{\mu\to\mu}(t)\right\rangle - \left\langle P_{\mu\to\mu}(t)\right\rangle^2}{\left\langle P_{\mu\to\mu}(t)\right\rangle^2} \sim O(D^0) \tag{4.19}$$

which cannot explain the increasing fluctuations with system size in Fig. 4.1.

So, what are we missing? It is important to stress that Eq. (4.16) only holds for the expectation value of $P_{\mu\to\nu}$ (we already took the Haar average) and does not necessarily account for the full statistics. Instead, a more careful treatment of the

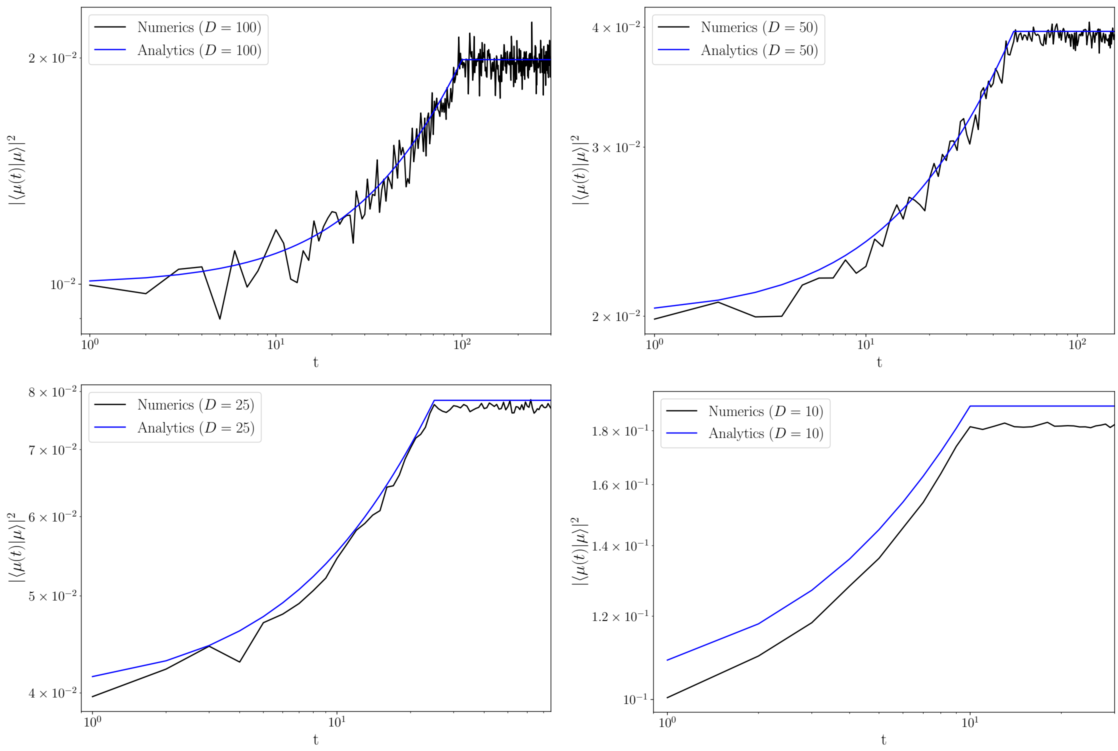

Figura 4.1: Two-point function $P_{\mu\to\mu}(t) = |\langle \mu(t)|\mu(t)\rangle|^2$ computed in the CUE for $D = 100, 50, 25, 10$ for 10^6 realizations.

2PF statistics requires working with a replicated version of the former generating function. We leave this question for future work.

4.2 Higher point functions and OTOCs

In this section, we briefly present how to generalize these computations to other correlation functions, such as

$$F(t) = \mathrm{tr}(\mathcal{A}(t)\mathcal{B}\mathcal{A}(t)\mathcal{B}) = \mathrm{tr}\left(\mathcal{U}^t \mathcal{A} \mathcal{U}^{\dagger^t} \mathcal{B}\, \mathcal{U}^t \mathcal{A} \mathcal{U}^{\dagger^t} \mathcal{B}\right) \tag{4.20}$$

in the CUE.

We could consider more general 4PFs, which can even help discuss the time dependence as before, but here we want to present a minimal pedagogical analysis of the method.

Diagrammatically, we now want to compute

$$\mathrm{tr}(\mathcal{A}(t)\mathcal{B}\mathcal{A}(t)\mathcal{B}) =$$

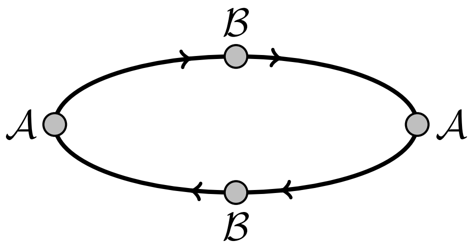

Since we have two contours, we will have, besides the causal structure, a replica structure to distinguish the two propagations. The corresponding discrete contour for this diagram is

$$\begin{array}{ccccccccccccc}
\boxed{0,+1} & \longrightarrow & \boxed{1,+1} & \longrightarrow & \cdots & \longrightarrow & \boxed{t,+1} & \longrightarrow & \boxed{t,-1} & \longrightarrow & \cdots & \longrightarrow & \boxed{0,-1} \\
 & & & & & & & & & & & & \downarrow \\
\boxed{0,+2} & \longleftarrow & \boxed{1,+2} & \longleftarrow & \cdots & \longleftarrow & \boxed{t,+2} & \longleftarrow & \boxed{t,-2} & \longleftarrow & \cdots & \longleftarrow & \boxed{0,-2} \\
\downarrow & & & & & & & & & & & & \\
\boxed{0,+1} & & & & & & & & & & & &
\end{array} \tag{4.21}$$

where we have added a new index corresponding to the "replica" contour.

The corresponding contour evolution is generated by

$$\mathcal{U}_{\mathrm{tw}} = \mathcal{P}_+ e^{i\phi_+} U T_+ + \mathcal{P}_- e^{-i\phi_-} U^\dagger T_- + \mathcal{A}\,\Pi_0\,\sigma^+_{ra}\sigma^x_{\mathrm{replica}} + \mathcal{B}\,\Pi_t\,\sigma^-_{ra} \tag{4.22}$$

where $\sigma^x_{\mathrm{replica}} = |1\rangle\langle 2| + |2\rangle\langle 1|$ is an operator swapping the replica contour. Next, we write

$$\mathcal{Z} = \mathrm{Det}(1 - \mathcal{U}_{\mathrm{tw}}), \tag{4.23}$$

using a Grassman representation, then the color-flavor transformation and integrating the fermions yields

$$\mathcal{Z}(\theta) = \int DB\ \exp\left[\mathrm{Tr}\log\left(1 - \kappa B^\dagger dB + \mathcal{B}\kappa\Pi_t B_T - \mathcal{A}\kappa B^\dagger \Pi_0 \sigma^x_{\mathrm{replica}}\right)\right] \tag{4.24}$$

where $\kappa = \frac{1}{1+B^\dagger B}$.

This can be further simplified by an analysis of the symmetries and evaluated in a perturbative $\frac{1}{D}$ expansion. However, the fact that the generating function becomes organized in a power series in $\frac{1}{D}$ means that we will have to go to very high orders to account for the full result. As a side comment, we mention the free probability formalism, which holds for correlations in the CUE in the large D limit and allows an elegant expansion in free cumulants [32, 31]. The connection between this free-probability and the Keldysh expansion is a very interesting connection that we leave for future work.

Capítulo 5

Quantum Sun Model

In the previous chapters, we have studied field-theoretical descriptions of random matrix theories at late times. Our primary motivation has been the observation that quantum-chaotic ergodic systems exhibit universal late-time behavior characteristic of random matrices. However, our discussion is far from complete, leaving several important questions open.

First, we would like to understand the mechanisms that lead to relaxation toward the late-time random-matrix regime. In other words, how does a system wash out its microscopic structure and flow toward a universal, almost structureless theory? In the language of Sec. 2.3.4, how are the "massive" degrees of freedom erased, allowing the Goldstone modes associated with causal symmetry breaking to dominate?

Second, in what precise sense do ergodic systems behave like random matrices? Is random-matrix universality merely a property of the spectrum, or does it extend to dynamical observables such as two-point correlation functions, OTOCs, etc?

Third, and related to the first point, what mechanisms can prevent a quantum system from reaching thermalization? In which language should we think about ergodic to non-ergodic transitions?

These are profound and challenging questions. To address them, a possible route could be to start from a microscopic many-body system and develop a framework capable of describing physics across all scales. This is, in many cases, too difficult.

A more practical and controlled approach is to begin with a RMT and introduce simple modifications or perturbations. In doing so, we obtain a minimal extension that remains analytically tractable and can serve as a benchmark for addressing some of the above questions. This is the approach we will adopt in this last chapter.

There are many possible ways to construct such models that extend RMTs and capture different physical regimes. Here, we will consider tensoring ancillary qubits weakly coupled to an RMT. This class of models has been previously proposed to study avalanche instabilities in the context of many-body localization

(MBL) [19, 33], and numerical investigations [34] have demonstrated that it exhibits an ergodic-to-non-ergodic transition. Nevertheless, a comprehensive analytical understanding of this model remains lacking.

This chapter is based on [2].

5.1 Model

The Quantum Sun is a (0+1)d (quantum mechanical) model consisting of a total of $N + M$ qubits. N of these qubits are going to be strongly ergodic, and we are going to model this by a $D \times D$ random matrix in the GUE ($D = 2^N$). The remaining M qubits are weakly coupled to this "bath" of N strongly interacting qubits. A sketch of the system is shown in Fig. 5.1. The total hamiltonian is $H = H_\text{B} + H_\text{S} + H_\text{BS}$, where

$$\begin{aligned} H_\text{B} &= \sum_{\alpha,\beta=1}^{D} H_{\alpha\beta} \left|\alpha\right\rangle \left\langle\beta\right| \otimes 1_{D_0} \qquad H_\text{S} = 1_D \otimes \sum_{a=1}^{M} \frac{h_a}{2} \hat{\sigma}_a^z, \\ H_\text{BS} &= \sum_{a=1}^{M} \sum_{\alpha,\beta=1}^{D} V_{\alpha\beta}^{(a)} \left|\alpha\right\rangle \left\langle\beta\right| \otimes \hat{\sigma}_a^+ + \text{h.c.} \end{aligned} \tag{5.1}$$

Here σ_a are the Pauli operators acting on the external spin $a = 1, \dots, M$, H is a $D \times D$ dimensional random hermitian matrix drawn from the GUE, and V is a general $D \times D$ dimensional complex matrix with random elements drawn from a Gaussian distribution

$$\langle H_{\alpha\beta} H_{\mu\nu}^* \rangle = \frac{\lambda^2}{D} \delta_{\alpha\mu} \delta_{\beta\nu}, \qquad \langle V_{\alpha\beta}^{(a)*} V_{\mu\nu}^{(b)} \rangle = \frac{v_a^2}{2D} \delta_{\alpha\mu} \delta_{\beta\nu} \delta^{ab}. \tag{5.2}$$

We can equivalently consider the Floquet version of this problem. In this case, time evolution is discrete and given by

$$\mathcal{U} = U\, V \qquad\qquad U = U_\text{Haar} \otimes e^{-iH_\text{S}} \qquad\qquad V = e^{-iH_\text{SB}} \tag{5.3}$$

where U_Haar is sampled from the Haar ensemble (CUE) and H_S and H_SB are given in Eq. (5.1).

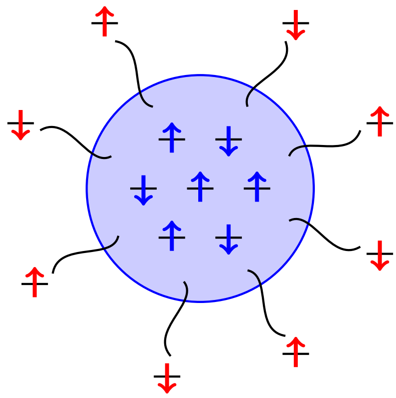

Figura 5.1: Sketch of model Eq. (5.1). M 'external' spins (red) weakly couple to N strongly interacting spins (blue) forming the bath.

5.1.1 Regimes

This system has many interesting regimes. Initially, it was proposed to be studied in the large M limit with N finite. By taking large random magnetic fields h_a, the idea was to consider the effect of embedding a small ergodic region in a strongly non-ergodic phase. The phenomenon people were interested in studying was avalanche instabilities, in which the "thermal bath" thermalized nearby spins, increasing in size and reducing its mean level spacing, making it a more powerful bath. As a result, it was argued that the formation of these rare small (N finite) ergodic regions could completely destabilize a many-body localized phase.

In this thesis, we are concerned with a different regime: the large-D limit with M finite. Our goal is to understand how thermalization is achieved and what deviations one can expect from random-matrix behavior, even in an ergodic setting.

Now, let us briefly describe the scales of interest. The Heisenberg time is (in units where $\lambda = 2$, as we employed in the previous chapters for GUE) $t_H = DD_0$. For early times, we expect all the external spin sectors to be decoupled, so $\mathrm{SFF(t)} = |Z(t)|^2 \sim D_0^2\, t$. For late times, we have the opposite limit: all spin sectors are completely coupled and H should behave similarly to a big $DD_0 \times DD_0$ random matrix, yielding a ramp $\mathrm{SFF}(t) \sim t$ and a plateau value of DD_0. The energy scale in which this relaxation is taking place can be estimated from the Fermi Golden Rule to be $\gamma = \frac{v^2}{2}$.

We are going to present a solution valid in the ergodic regime $D\gamma \gg 1$, where the "massive" modes relax before any plateau physics, giving place to a well-defined RMT behavior before the Heisenberg time. We will also need to work in the weakly coupled regime $\gamma \ll 1$, to avoid second loop corrections.

5.2 Perturbative Solution - Keldysh formalism

We will start by working in the Keldysh formalism. This will allow us to present a simple diagrammatic solution of the relaxation to the late-time ergodic behavior.

We will focus on the single-external-spin case, leaving the straightforward generalization to multiple spins (M finite) to the end.

5.2.1 Field Theory

To write a generating function, we follow Sec. 2.4, with almost no additional complications. We get

$$\mathcal{Z}(\theta) = \int D\psi \ \exp\Big(-\bar{\psi}\psi + \bar{\psi}^{+} e^{i\phi_+} UVT_+\psi_+ + \bar{\psi}^{-} e^{-i\phi_-} V^\dagger U^\dagger T_-\psi_-\Big) \tag{5.4}$$

with Grassman variables $\psi = \psi^{\pm}_{a\alpha}$. We next perform the Haar average by doing a color-flavor transformation, yielding an integral over the matrix fields $B = B_{ab,nm}$ ($a, b = 1, \ldots, D_0$; $n, m = 1, \ldots, t$). We find

$$\mathcal{Z} = \int DB \ \exp\Big(-\operatorname{Tr}\log\Big(1 + B^\dagger B\Big) + \operatorname{Tr}\log\Big(1 + VB_T V^\dagger B^\dagger\Big)\Big) \tag{5.5}$$

where we have introduced $B_T = e^{i\phi} T_+ B T_-$ and the traces Tr are over the $D \times D_0$ space involving external and dot indices.

Next, we will approximate the interaction. By expanding to leading order in $\gamma = \frac{v^2}{2}$, $V = e^{-iH_{\mathrm{SB}}} \approx 1 - iH_{\mathrm{SB}} - \frac{1}{2} H^2_{\mathrm{SB}}$, we get

$$\mathcal{Z} = \int DB \ \exp\Big[-D\operatorname{Tr}\Big(\kappa B^\dagger \mathbb{d} B\Big) + D\gamma \operatorname{Tr}\Big(\kappa B^\dagger [\sigma^+, B] \kappa B^\dagger [\sigma^-, B]\Big)\Big] \tag{5.6}$$

where we have introduced $\kappa = \frac{1}{1+B^\dagger B}$ and the matrix operator

$$\mathbb{d} = d + \gamma(1 - \mathcal{O}), \tag{5.7}$$

with $\mathcal{O}$ an operator acting on the the matrix fields as

$$\mathcal{O}B = \sigma^+ B \sigma^- + \sigma^- B \sigma^+. \tag{5.8}$$

What is the meaning of Eq. (5.6)? The first term corresponds to a generalization of the structureless (massless) RMT propagator to the case of a non-trivial trivial external spin structure. This non-trivial propagator will organize the theory into a set of massive modes that will decay at late times. One of the modes will remain massless, yielding late-time RMT physics; see the next section. The second term corresponds to a novel interaction that will not appear in the semiclassical theory.

5.2.2 Diagrammatic interpretation

In this section, we would like to focus on the semiclassical theory

$$\mathcal{Z}_{\rm sc} = \int DB\, e^{-D\,\mathrm{Tr}\left(B^\dagger \mathbb{d} B\right)} \tag{5.9}$$

and discuss the structure of the propagator $\mathbb{d} = d + \gamma(1 - \mathcal{O})$.

The propagator contains two new terms. First, it includes a constant self-energy γ that will affect all the modes B_{ab} equally. This is the usual decay of the 2PF due to the Fermi-Golden rule, as depicted in Fig. .

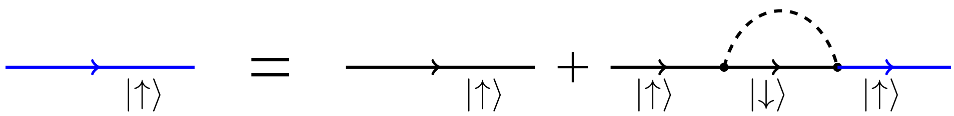

Figura 5.2: Lowest order self-energy correction for the propagator of the state $|\!\uparrow\rangle$.

The third term contains the operator $\mathcal{O} = \sigma_L^+\sigma_R^- + \sigma_L^-\sigma_R^+$ and corresponds to a vertex correction. Let's think of B_{ab} as describing the propagation of a retarded (a) and advanced (b) external spin state. Then, this term amounts to an interaction that simultaneously swaps both spins, as depicted in Fig. 5.3. Thus, the modes $B_{\uparrow\downarrow}$ and $B_{\downarrow\uparrow}$ will not be affected by it, while $\mathcal{O}B_{\uparrow\uparrow} = B_{\downarrow\downarrow}$ and $\mathcal{O}B_{\downarrow\downarrow} = B_{\uparrow\uparrow}$. The effect of this vertex correction is to favor "paths" where the scattering processes in the retarded and advanced lines are identical, but traversed in reverse order. Physically, this is due to phase cancellation between the advanced and retarded scattering paths (cancellation of the destructive interference) and is the origin of the long-lived (massless) ergodic mode.

We can diagonalize the vertex correction operator $\mathcal{O}$ by simply working in the Pauli basis

$$\mathcal{O}\sigma^\mu = \sigma_\mu v^\mu \qquad \lambda_\mu = 1, 0, 0, -1 \tag{5.10}$$

where we are using the convention $\sigma^0 = 1_2$ and σ^i are the usual Pauli matrices for

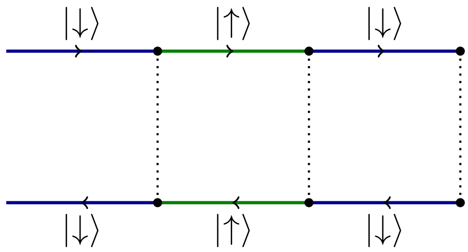

Figura 5.3: Vertex corrections due to $\mathcal{O} = \sigma_L^+ \sigma_R^- + \sigma_L^- \sigma_R^+$ involved in the propagator $\mathbb{d}^{-1}$.

$i = 1, 2, 3$. As a result, the theory contains four modes:

$$B = \frac{1}{\sqrt{2}} \sum_\mu B_\mu \, \sigma^\mu \qquad\qquad \epsilon_\mu = 0, \gamma, \gamma, 2\gamma \tag{5.11}$$

where the factor of $\frac{1}{\sqrt{2}}$ is there to give the correct normalization: $\frac{1}{2}\,\mathrm{tr}(\sigma^\mu \sigma^\nu) = \delta^{\mu\nu}$.

We can now evaluate the generating function as before,

$$\mathcal{Z}_{\mathrm{sc}} = \int DB \;\exp\left(-\sum_\mu \mathrm{tr}\Big(B_\mu^\dagger (1 - e^{-\epsilon_\mu + i\phi} \mathcal{T}) B_\mu \Big) \right) \tag{5.12}$$

Therefore,

$$\begin{aligned} \mathcal{Z}(\theta) &= \prod_\mu \det\Big(1 - e^{-\epsilon_\mu + i\phi}\mathcal{T}\Big)^{-1} = \prod_\mu \exp\Big(-t\,\mathrm{tr}\log\Big(1 - e^{i\phi - \epsilon_\mu}\mathcal{T}\Big)\Big) \\ &= \exp\left(-t \sum_\mu \mathrm{tr}\log\Big(1 - e^{i\theta - \epsilon_\mu t}\Big)\right) = \exp\left(\sum_\mu t e^{-\epsilon_\mu t}\, e^{i\theta} + O(e^{2i\theta})\right) \end{aligned} \tag{5.13}$$

As a result,

$$\mathrm{SFF}(t) = t \sum_\mu e^{-\epsilon_\mu t} \tag{5.14}$$

As anticipated, for early times all external spin sectors are decoupled and $\mathrm{SFF}(t) \sim D_0^2\, t$ but for late times all sectors are coupled, and the system behaves like a large random matrix, $\mathrm{SFF}(t) \sim t$.

Thus, the emergence of the late-time RMT behavior can be easily understood as follows. The theory has a set of modes describing the forward and backward propagation of states. Interference from scattering processes will produce exponential decay in the propagation of these modes. There can be a partial phase cancellation between the retarded and advanced lines, as long as the scattering processes are traversed in the same order, which manifests in the field theory as a vertex correction. This yields a spectrum of masses ϵ_μ which will always contain a massless mode corresponding to paths traversing the same process in both retarded and advanced lines: this is our aforementioned Goldstone ergodic mode.

The generalization to multiple spins is straightforward. We can diagonalize the propagator in the tensor basis

$$B = \frac{1}{2^{M/2}} \sum_{\mu_1,\mu_2,\cdots,\mu_M} B_\mu \, \sigma^{\mu_1} \otimes \sigma^{\mu_2} \otimes \cdots \sigma^{\mu_M} \tag{5.15}$$

yielding masses $\epsilon_{\mu_1,\mu_2,\cdots,\mu_M} = \sum_{a=1}^{M} \epsilon_{\mu_a}$.

5.2.3 SFF Statistics

The generalization of the semiclassical calculation to higher moments is also straightforward. We get

$$\begin{aligned} \mathcal{Z}_n &= \prod_\mu \exp\Big(-t \operatorname{tr} \log\Big(1 - e^{i\Phi - \epsilon_\mu} \otimes \mathcal{T}\Big)\Big) \\ &= \exp\left(t \sum_\mu e^{-\epsilon_\mu t} \operatorname{tr} e^{i\Phi t}\right) = \exp\Big(\mathrm{SFF}(t) \operatorname{tr} e^{i\Phi t}\Big) \end{aligned} \tag{5.16}$$

where $\Phi = \phi_+^{s_+} - \phi_-^{s_-}$. Which yields the Gaussian statistics

$$\langle \mathrm{SFF}^n(t) \rangle = n! \, \langle \mathrm{SFF(t)} \rangle^n . \tag{5.17}$$

5.3 Field Theory - Efetov's Sigma Model

One of the main points that we missed in the previous calculation is the emergence of the plateau. In this section, we follow Efetov's approach, described Sec. 2.3, to see the effect of these massive modes in the late-time physics.

5.3.1 Deriving the Field Theory

We start by introducing the generating function and expressing it as integral over complex and Grassmann variables

$$\mathcal{Z}(\vec{z}) = \left\langle \frac{\det(z_1 - H)\det(z_2 - H)}{\det(z_3 - H)\det(z_4 - H)} \right\rangle = \left\langle \int d\psi \, e^{i\bar{\psi}(z-H)\psi} \right\rangle \tag{5.18}$$

where $\psi = \psi_{\alpha a}$ are $D \times D_0 \times 2 \times 2$ graded supervectors. Note that Greek letters correspond to spin-dot subindices while Latin letters correspond to external spin states. To compute the SFF, we will employ a source z independent of both external spins and spin-dot indices and given by: $z = \frac{1}{2}\Lambda(\omega + \alpha k)$. We then disorder average, perform a Hubbard-Stratonovich transformation and integrate the ψ fields to find:

$$\mathcal{Z}(z) = \int DQ \, e^{S[Q]}, \qquad S[Q] = \frac{D}{2}\mathrm{Str}(Q^2) - \mathrm{STr}\log(z - H_S - H_{\mathrm{SB}} + i\lambda Q) \tag{5.19}$$

Note that we employed STr instead of Str to emphasize that it is also a trace over the ergodic dot.

Now, let us simplify this model. First, we will fix the energy scale by setting $\lambda = 2$, and focus on the case $h_a = 0$ (no magnetic field). Second, we will work in the large D limit and the weak coupling regime, giving two expansion parameters: $\frac{1}{D}$ and $\gamma_a = \frac{v_a^2}{2}$.

Thus, we perform a stationary phase analysis to find the most relevant degrees of freedom for this theory. Working close to the center of the spectrum $z \sim \frac{1}{D}$, we find that the saddle equation is given by

$$Q^2 = 1 \tag{5.20}$$

This is the characteristic non-linear sigma model constraint in Efetov's Sigma Model, Eq. (2.27), determining the manifold of low-energy degrees of freedom.

Using Eq. (5.20), we can expand to find the following effective action

$$S[Q] = \frac{iD}{2}\,\mathrm{Str}(zQ) - \frac{D}{4}\sum_{j=1}^{M}\gamma_j\,\mathrm{Str}(Q\sigma_j^+ Q\sigma_j^-) \tag{5.21}$$

where $\gamma_j = \frac{v_j^2}{2}$.

5.3.2 Semiclassical Calculation

Now, we will proceed to evaluate this semiclassically. We will focus on the single spin case because the generalization to higher spins is straightforward.

As we have learnt in Sec. 2.3, there are two special saddles: Standard ($Q_0 = \Lambda$) and Andreev-Altshuler ($Q_0 = \Lambda k$), which yield the SFF in RMT. They will be of special interest in the present.

Our discussion in Sec. 3.2 may tempt us to consider even more saddles. As we discussed there, the presence of a replica structure allows for a novel set of saddles, which ultimately gives important contributions to the second moment. Could it be that the same is happening here? A careful analysis shows that single permutations of the standard saddle actually carry a finite action contribution, $D\gamma$. This means that they will not become relevant as long as we are probing ergodic regimes, where $\gamma^{-1} \ll t_{\mathrm{H}}$. It is a question of great interest to determine the effect of these saddles in this "non-ergodic" regime. This is part of ongoing work and will not be discussed in this thesis.

Standard Saddle

We start by considering fluctuations around the Standard saddle, $Q = T\Lambda T^{-1}$. We employ the same exponential parametrization as in Eq. (2.31), where one needs to take into account the external spin structure. That is, for example, $w = w_{ab}$ is a $D_0 \times D_0$ matrix.

The interaction term then reads

$$-D\frac{\gamma}{4}\mathrm{Str}(Q\sigma^{+}Q\sigma^{-}) = -\frac{D\gamma}{2}\,\mathrm{Str}(W^{2} - 2\sigma^{+}W\sigma^{-}W) = -D\gamma\,\mathrm{Str}(\tilde{B}B - \tilde{B}\,\mathcal{O}B) \tag{5.22}$$

where we have introduced the operator $\mathcal{O}$ acting on matrices as before, $\mathcal{O}B = \sigma^{+}B\sigma^{-} + \sigma^{-}B\sigma^{+}$.

By writing the pion fields in this basis: $B = \sum_\mu B_\mu v^\mu$, $\tilde{B} = \sum_\mu \tilde{B}_\mu v^\mu$, with $B_\mu, \tilde{B}_\mu$ 2×2 supermatrices, we can write the semiclassical theory as follows

$$S = iD\left(2\alpha + \sum_{\mu}\mathrm{str}((\omega + i\epsilon_\mu + \alpha k)(\tilde{B}_\mu B_\mu + B_\mu \tilde{B}_\mu))\right) \tag{5.23}$$

where $\epsilon_\mu = 0, \gamma, \gamma,\ 2\gamma$. As a side remark, we note that if we introduce a magnetic field, $h \neq 0$, the only effect would be to modify some of the masses: $\epsilon_\mu = 0, \gamma + ih, \gamma - ih, 2\gamma$.

Finally, we can perform the Gaussian integrals over complex and Grasmann variables, yielding the standard saddle contribution to the generating function

$$\mathcal{Z}_0(\omega, \alpha) = e^{i\alpha t_H} \prod_{\mu} \frac{(\omega + i\epsilon_\mu)^2}{(\omega + i\epsilon_\mu)^2 - \alpha^2} \tag{5.24}$$

where $t_H = 2D$ and $\epsilon_\mu = 0, \gamma, \gamma, 2\gamma$. As a simple check, we observe that $\mu = 0$ reproduces the RMT result, Eq. (2.34).

Andreev-Altshuler Saddle

We now evaluate the contribution corresponding to the AA saddle ($Q_0 = \Lambda k$). We can perform the same trick that we did in Sec. 2.3.3, which consists of first performing a global rotation $Q' = T_0^{-1} Q T_0$ such that the saddle is mapped to $Q'_{AA} = T_0^{-1} k \tau_3 T_0 = \tau_3$. Since the transformation commutes with the external spins and it leaves the action measure invariant, the only effect is to modify the sources

$$z = \frac{1}{2}(\omega + \alpha k)\tau_3 \;\rightarrow\; z' = \frac{1}{2}(\alpha + \omega k)\tau_3 \tag{5.25}$$

It then immediately follows that the AA saddle contributes to the generating function by

$$\mathcal{Z}_{AA}(\omega, \alpha) = \mathcal{Z}_0(\alpha, \omega) = e^{i\omega t_H} \prod_{\mu} \frac{(\alpha + i\epsilon_\mu)^2}{(\alpha + i\epsilon_\mu)^2 - \omega^2} \tag{5.26}$$

Spectral Form Factor

We are now ready to compute the SFF. After taking the two derivatives, we find

$$R_2(\omega) = -\mathrm{Re}\, \partial_\alpha^2 \mathcal{Z} = \mathrm{Re} \left(-2t_H^2 + \sum_{\mu} \frac{1}{(\omega + i\epsilon_\mu)^2} - 2\frac{e^{i\omega t_H}}{\omega^2} \prod_{\mu \neq 0} \frac{\epsilon_\mu^2}{\omega^2 + \epsilon_\mu^2} \right) \tag{5.27}$$

Evaluating the Fourier transform for $t > 0$ gives[1]

$$\begin{aligned}
&\mathrm{SFF}(t) = t\sum_{\mu} e^{-\epsilon_\mu t} - (t - t_H)\theta(t - t_H) - \sum_{\mu\neq 0} \frac{\mathcal{K}(\epsilon_\mu)}{2\epsilon_\mu}\left(e^{-\epsilon_\mu|t-t_H|} + e^{-\epsilon_\mu(t+t_H)}\right) \\
&\mathcal{K}(\epsilon_\mu) = \prod_{\nu\neq\mu,0} \frac{\epsilon_\nu^2}{\epsilon_\nu^2 - \epsilon_\mu^2} \qquad \epsilon_\mu = 0, \gamma, \gamma, 2\gamma \qquad t_H = 2D
\end{aligned} \tag{5.28}$$

We obtain three pieces. First, the standard saddle gives the decay of the initial ramp (SFF $\sim 4t$) to the full-RMT ramp (SFF $\sim t$), in agreement with our Keldysh result, Eq. (5.14). Second, we have the usual RMT plateau contribution coming from the AA saddle, enforcing SFF $\to 2D$ at late times. The third and final term is new and owes its presence to the massive modes. This effect corresponds to the rounding of the singular behavior at $t = t_H$ observed in RMT, Fig. 2.1. This occurs because $\sum_{\mu\neq 0}\mathcal{K}(\epsilon_\mu) = -1$, making $\partial_t K$ continuous at the Heisenberg time.

Our results are compared with numerics in Fig. 5.4, and we find excellent agreement without any fitting parameters. One of the most surprising findings is that our analytical calculations capture the precise rounding of the SFF at $t = t_H$. This remarkable agreement strongly suggests that the system is semiclassically exact, which we will verify in Sec. 5.4.

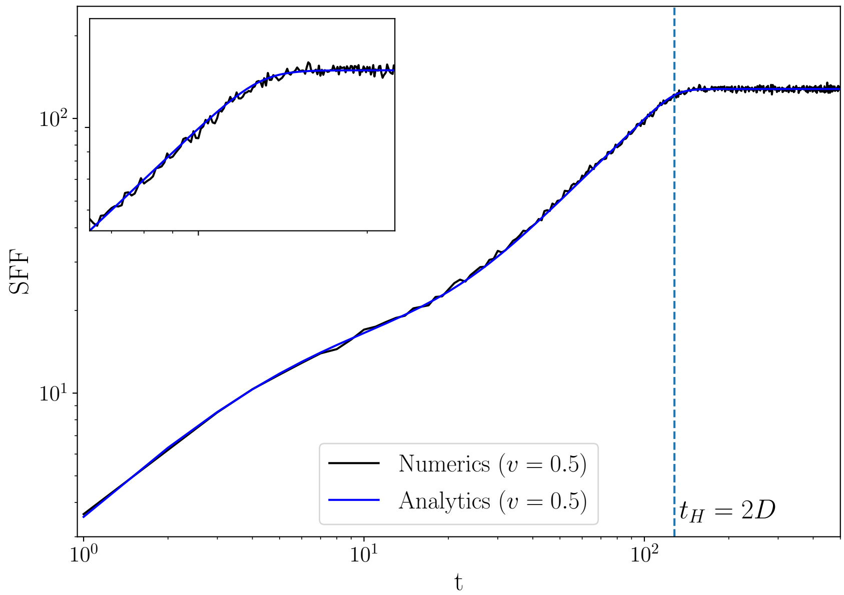

Figura 5.4: Spectral Form Factor for a single spin coupled to a spin-dot of size $D = 64$. No fitting parameters were used in the analytical expression.

[1] It is important to recall that we must use $\omega = \omega + i0^+$ when there is no mass.

There is, however, a strange feature that will appear for sufficiently small couplings. To illustrate it, consider the single-level case of this expression ($\epsilon_\mu = 0, \gamma$)

$$\mathrm{SFF}(t) = t - (t - t_{\mathrm{H}})\theta(t - t_{\mathrm{H}}) + t\, e^{-\gamma t} - \frac{1}{2\gamma}(e^{-\gamma|t-t_{\mathrm{H}}|} + e^{-\gamma(t+t_{\mathrm{H}})}) \tag{5.29}$$

As $\gamma \to 0$, we observe that the second term becomes increasingly larger, to the point that it makes the SFF negative. Of course, this is not physical behavior, suggesting some kind of non-ergodic behavior. We leave a more detailed study of this regime for future work.

5.4 Semiclassical Exactness in the Quantum Sun

In this last section, we will check that the Quantum Sun sigma model, Eq. (5.21), indeed enjoys semiclassical exactness to leading order in γ. To do so, we need first to generalize our discussion of Sec. 2.4.3 by introducing propagators and contraction rules in the presence of external spin structure.

Propagator and contraction rules

In the semiclassical theory, the propagator is

$$\Pi^{\mu,\nu}_{n,m} = \left\langle B^{\mu}_{n_+,n_-} B^{\nu\dagger}_{m_-,m_+} \right\rangle \tag{5.30}$$

and satisfies

$$D(\Pi)^{\mu\nu}_{n,m} = \Pi^{\mu\nu}_{n,m} - e^{i\phi-\epsilon\mu}\, \Pi^{\mu\nu}_{n-1,m} = \delta_{n,m}\delta^{\mu\nu} \tag{5.31}$$

If we work to the lowest order in γ, it is simply given by

$$\begin{aligned} \Pi^{\mu,\nu}_{n,m} &= \frac{1}{D}\delta^{\mu\nu}\delta_{\Delta n,\Delta m}\Theta(\bar{n}-\bar{m})\, k_\mu(\bar{n}-\bar{m}) \\ k_\mu(\bar{n}) &= e^{(i\phi-\epsilon_\mu)\bar{n}} \end{aligned} \tag{5.32}$$

Now, we want to look at contraction rules. One could think that the presence of external spin structure would modify the RMT contraction rules, Eq. (5.33).

However, a short calculation shows that this is not the case

$$\begin{aligned} \left\langle \operatorname{Tr}\left(A(\mathbb{d}B)CB^\dagger\right)\right\rangle &= \frac{1}{D}\operatorname{Tr}(A)\operatorname{Tr}(C) \\ \left\langle \operatorname{Tr}(A(\mathbb{d}B))\operatorname{Tr}\left(CB^\dagger\right)\right\rangle &= \frac{1}{D}\operatorname{Tr}(AC) \end{aligned} \tag{5.33}$$

provided that we also trace over external spins.

Semiclassical Exactness

Now, we are ready to verify semiclassical exactness. Let us recall that our action of interest is

$$S = -D\operatorname{Tr}\left(\kappa B^\dagger \mathbb{d}B\right) + D\gamma\operatorname{Tr}\left(\kappa B^\dagger[\sigma^+, B]\kappa B^\dagger[\sigma^-, B]\right) \tag{5.34}$$

where $\kappa = \frac{1}{1+B^\dagger B}$.

The first class of terms is a straightforward generalization of the RMT case, Eq. (2.64). We thus know that the higher-loop contributions corresponding to this term immediately cancel. For instance,

$$D^2\left\langle \operatorname{Tr}\left(B^\dagger BB^\dagger \mathbb{d}B\right)\operatorname{Tr}\left(B^\dagger BB^\dagger \mathbb{d}B\right)\right\rangle \to 2D\left\langle \operatorname{Tr}\left(B^\dagger BB^\dagger\right)\operatorname{Tr}\left(BB^\dagger \mathbb{d}B\right)\right\rangle \tag{5.35}$$

Now, let us look at the new term:

$$S_{\text{int}} = \gamma\operatorname{Tr}\left(\frac{1}{1+B^\dagger B}B^\dagger[\sigma^+, B]\frac{1}{1+B^\dagger B}B^\dagger[\sigma^-, B]\right) \tag{5.36}$$

We introduce the diagrammatic notion as follows. Introduce polygons where B and $B^\dagger$ lie at the consecutive vertices. Operators $\sigma^\pm$ are inserted at the edges of the polygons and $\mathbb{d}$ at the corresponding vertices. For example,

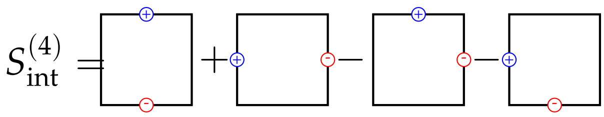

Higher orders are similar. For example, for $S^{(6)}_{\text{int}}$ we will have hexagons such as

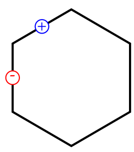

where the global sign is given by the relative "parity" between the + and − gates.

We note the contraction $S_0^{(4)}$ with $S_{\text{int}}^{(4)}$, we always get a diagram in $S_{\text{int}}^{(6)}$. For example,

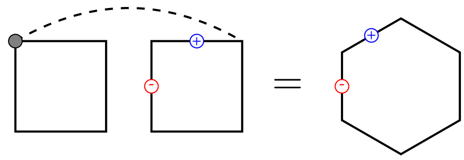

In fact, it is not hard to check that

$$\left\langle S_{\text{int}}^{(6)} \right\rangle + \left\langle S_{\text{int}}^{(4)} S_0^{(4)} \right\rangle = 0 \tag{5.37}$$

Note that there is no factor of 2 since $e^{S_{\text{int}}^{(4)} + S_0^{(4)}} \to S_{\text{int}}^{(4)} S_0^{(4)}$.

But, what about terms such as $\left\langle S_{\text{int}}^{(4)} S_{\text{int}}^{(4)} \right\rangle$? Since we are working to leading order in γ, we do not have to worry about them. We can do some power counting to check:

$$\left\langle S_{\text{int}}^{(4)} S_{\text{int}}^{(4)} \right\rangle \sim (D\gamma)^2 D^{-4} \sim \frac{\gamma^2}{D^2}$$

If we wanted to do a consistent calculation to second order in γ, we would also have to consider order γ^2 in S^6:

$$\text{second order } \left\langle S^{(6)} \right\rangle \sim D\gamma^2 D^{-3} \sim \frac{\gamma^2}{D^2}$$

Going back to our computation to lowest order in γ in the action, we may wonder what happens to higher orders in B. For instance,

$$e^{S_0^{(4)} + S_0^{(6)}} e^{S_{\text{int}}^{(4)} + S_{\text{int}}^{(6)} + S_{\text{int}}^{(8)}} \to S_{\text{int}}^{(8)} + S_{\text{int}}^{(6)} S_0^{(4)} + S_0^{(6)} S_{\text{int}}^{(4)} + \frac{1}{2} S_0^{(4)} S_0^{(4)} S_{\text{int}}^{(4)} \tag{5.38}$$

One can also check that

$$\left\langle S_{\text{int}}^{(8)} + S_{\text{int}}^{(6)} S_0^{(4)} + S_0^{(6)} S_{\text{int}}^{(4)} + \frac{1}{2} \left(S_0^{(4)} \right)^2 S_{\text{int}}^{(4)} \right\rangle = 0 \tag{5.39}$$

Therefore, to first order in γ, we observe a cancellation of all diagrams and the theory is semiclassically exact. This result also extends to multiple spins.

Capítulo 6

Conclusions

Understanding the thermalization of quantum systems from a universal perspective is not only a rich conceptual challenge but also key to understanding non-ergodic phases and addressing deep questions in quantum chaos and holography.

In this regard, one of the key insights is the notion of random matrix universality. At sufficiently late times, ergodic quantum systems exhibit correlations reminiscent of those of random matrices in the appropriate symmetry class. One quantitative diagnostic of this is the two-level correlation function and its close cousin, the spectral form factor. The universal structure of these observables serves as a diagnostic of thermalization, making it one of the central quantities in quantum chaos.

In this thesis, we employed the Quantum Sun Model to understand the emergence of RMT behavior as follows. Quantum chaotic correlations involve interacting retarded and advanced degrees of freedom, which the system organizes into a set of massive modes arising from interference processes in scattering. The mass spectrum is determined by both self-energies and vertex corrections, which result from phase cancellations between retarded and advanced degrees of freedom. Importantly, the existence of a massless (Goldstone) mode is protected by causal-symmetry breaking, ensuring the late-time ergodic (RMT) behavior.

From a quantitative perspective, causal-symmetry breaking implies that the effective theory is governed by two distinct saddles. The standard saddle accounts for the ramp behavior of spectral correlations: the initially decoupled sectors acquire a finite mass and decay, leaving only the full-RMT ramp associated with the massless mode. The Andreev–Altshuler saddle, by contrast, dominates near and after the Heisenberg time, giving rise to the plateau in the spectral form factor. Together, these two saddles describe the universal content of quantum chaotic systems.

One of our interesting findings is the precision of the semiclassical theory in describing the ergodic regime in the Quantum Sun. We verified this semiclassical exactness and discussed its connection with non-Gaussian statistics. Remarkably, we found that these non-Gaussian statistics are captured by a set of new saddles that generalize the Andreev–Altshuler saddle in a replicated target manifold.

Looking ahead, there are several interesting directions. On the one hand, we expect the notion of random matrix universality to extend across various correlation functions, not just the low-energy spectrum. It would be interesting to understand the effects of massive modes on correlation functions and whether they can have long-lasting effects, leading to deviations from random-matrix behavior even in ergodic regimes.

Secondly, our analysis has been primarily centered around the ergodic phase in the Quantum Sun. Here, we found that semiclassical exactness is a key property allowing us to describe an interacting theory as if it were free. We observed that as we reduced the coupling strength, our semiclassical calculation failed. However, we also identified the presence of a set of new saddles, analogous to those leading to non-Gaussian statistics, which become relevant in this regime. Understanding the effect of these new saddles, and whether semiclassical exactness breaks down as we reduce the coupling, may lead us to a richer understanding of non-ergodic phases.

Lastly, it would be interesting to develop the framework to extend our analysis to a large number of external spins, which could provide further analytical evidence for the existence of avalanche instabilities in Many-Body localized systems.

Apêndice A

Connection with the Sigma Model

In this Appendix, we briefly show the equivalence between the Keldysh formalism and Efetov's method in the Quantum Sun. We start by considering Eq. (5.5) and we introduce the retarded/advanced structure as

$$Q(B,B^\dagger) = \begin{pmatrix} 1 & B \\ -B^\dagger & 1 \end{pmatrix} \begin{pmatrix} 1 & 0 \\ 0 & -1 \end{pmatrix} \begin{pmatrix} 1 & B \\ -B^\dagger & 1 \end{pmatrix}^{-1} \equiv T\Lambda T^{-1}, \tag{A.1}$$

We can now write

$$\begin{aligned} \operatorname{Tr}\log\left(1 + BB^\dagger\right) &= \operatorname{Tr}\log\left(1 - \begin{pmatrix} 0 & B \\ -B^\dagger & 0 \end{pmatrix}\right) \\ \operatorname{Tr}\log\left(1 + V^\dagger B^\dagger V B\right) &= \operatorname{Tr}\log\left(1 - \begin{pmatrix} V & 0 \\ 0 & V^\dagger \end{pmatrix} \begin{pmatrix} 0 & B \\ -B^\dagger & 0 \end{pmatrix}\right) \end{aligned} \tag{A.2}$$

and using the fact that

$$1 - \begin{pmatrix} 0 & B \\ -B^\dagger & 0 \end{pmatrix} = 2\left(1 + Q\Lambda\right)^{-1}, \tag{A.3}$$

Thus, we get

$$\mathcal{Z} = \int DB\, \exp\left[\operatorname{Tr}\log\left(\frac{1+\mathcal{V}}{2} + \frac{1-\mathcal{V}}{2} Q\Lambda\right) - \operatorname{Tr}\left(\frac{1}{1+B^\dagger B} B^\dagger \partial B\right)\right] \tag{A.4}$$

where we have introduced $\mathcal{V} = \begin{pmatrix} V & 0 \\ 0 & V^\dagger \end{pmatrix} = e^{-i\Lambda X}$.

Alternatively, we can write this as follows

$$\mathcal{Z} = \mathcal{N} \int DB\, \exp\left(\operatorname{Tr}\log\left(1 + \frac{1-\mathcal{V}}{1+\mathcal{V}} Q\Lambda\right) - \operatorname{Tr}\left(\frac{1}{1+B^\dagger B} B^\dagger \partial B\right)\right) \tag{A.5}$$

where $\mathcal{N} = \exp\left[\operatorname{Tr}\log\left(\frac{1+\mathcal{V}}{2}\right)\right]$ is a non-trivial constant. Note that the action contribution at the standard saddle ($Q_T = \Lambda$) cancels this $\mathcal{N}$. In other words, $\mathcal{N} = e^{-S_d[Q=\Lambda]}$ where

$$S_d[Q] = \mathrm{Tr}\log\left(1 + \frac{1-\mathcal{V}}{1+\mathcal{V}} Q\Lambda\right) \tag{A.6}$$

Finally, we can expand this dynamical term. To leading order in γ

$$\begin{aligned}
S_d[Q] &= \frac{D\gamma}{4}\mathrm{Tr}\left(Q\sigma^+ Q\sigma^-\right) + O(D\gamma^2) \\
&= \frac{D\gamma}{4}\mathrm{Tr}\Big((1-BB^\dagger)\frac{1}{1+BB^\dagger}\sigma^+(1-BB^\dagger)\frac{1}{1+BB^\dagger}\sigma^- + 4B\frac{1}{1+B^\dagger B}\sigma^+ B^\dagger \frac{1}{1+BB^\dagger}\sigma^- + \\
&\qquad (1-B^\dagger B)\frac{1}{1+B^\dagger B}\sigma^+(1-B^\dagger B)\frac{1}{1+B^\dagger B}\sigma^- + 4B\frac{1}{1+B^\dagger B}\sigma^- B^\dagger \frac{1}{1+BB^\dagger}\sigma^+\Big)
\end{aligned}$$

With a bit of algebra, one can show that this reproduces Eq. (5.6).

Referências

[1] A. Altland, F. Divi, T. Micklitz, S. Pappalardi, and M. Rezaei, Phys. Rev. Res. **7**, 033138 (2025).

[2] A. Altland, F. Divi, T. Micklitz, and M. Rezaei, arXiv preprint arXiv:2512.13803 https://doi.org/10.48550/arXiv.2512.13803 (2025).

[3] A. Altland and B. D. Simons, *Condensed matter field theory* (Cambridge university press, 2010).

[4] D. A. Abanin, E. Altman, I. Bloch, and M. Serbyn, Reviews of Modern Physics **91**, 021001 (2019).

[5] A. Altland and J. Sonner, SciPost Physics **11**, 034 (2021).

[6] P. Sierant, M. Lewenstein, A. Scardicchio, L. Vidmar, and J. Zakrzewski, Reports on Progress in Physics **88**, 026502 (2025).

[7] J. S. Cotler, G. Gur-Ari, M. Hanada, J. Polchinski, P. Saad, S. H. Shenker, D. Stanford, A. Streicher, and M. Tezuka, Journal of High Energy Physics **2017**, 1 (2017).

[8] J. Cotler, N. Hunter-Jones, J. Liu, and B. Yoshida, Journal of High Energy Physics **2017**, 1 (2017).

[9] G. Penington, S. H. Shenker, D. Stanford, and Z. Yang, Journal of High Energy Physics **2022**, 1 (2022).

[10] P. Saad, S. H. Shenker, and D. Stanford, arXiv preprint arXiv:1806.06840 (2018).

[11] S. H. Shenker and D. Stanford, Journal of High Energy Physics **2014**, 1 (2014).

[12] J. Maldacena, S. H. Shenker, and D. Stanford, Journal of High Energy Physics **2016**, 1 (2016).

[13] F. Haake, *Quantum signatures of chaos* (Springer, 1991).

[14] K. Efetov, *Supersymmetry in disorder and chaos* (Cambridge university press, 1999).

[15] A. Altland, K. W. Kim, and T. Micklitz, arXiv preprint arXiv:2509.06028 (2025).

[16] B. L. Altshuler, Y. Gefen, A. Kamenev, and L. S. Levitov, Physical review letters **78**, 2803 (1997).

[17] I. V. Gornyi, A. D. Mirlin, and D. G. Polyakov, Physical review letters **95**, 206603 (2005).

[18] D. M. Basko, I. L. Aleiner, and B. L. Altshuler, Annals of physics **321**, 1126 (2006).

[19] W. De Roeck and F. Huveneers, Physical Review B **95**, 155129 (2017).

[20] E. P. Wigner, in *The Collected Works of Eugene Paul Wigner: Part A: The Scientific Papers* (Springer, 1993) pp. 524–540.

[21] F. Divi, J. Murugan, and D. Rosa, Phys. Rev. B **111**, 075138 (2025).

[22] F. J. Dyson, Journal of Mathematical Physics **3**, 166 (1962).

[23] A. Andreev and B. Altshuler, Physical review letters **75**, 902 (1995).

[24] M. R. Zirnbauer, arXiv preprint chao-dyn/9810016 (1998).

[25] A. Altland, S. Gnutzmann, F. Haake, and T. Micklitz, Reports on Progress in Physics **78**, 086001 (2015).

[26] A. Altland and A. Kamenev, Physical review letters **85**, 5615 (2000).

[27] S. Müller, S. Heusler, A. Altland, P. Braun, and F. Haake, New Journal of Physics **11**, 103025 (2009).

[28] C. Itzykson and J.-B. Zuber, Journal of Mathematical Physics **21**, 411 (1980).

[29] Y. V. Fyodorov and E. Strahov, Nuclear Physics B **630**, 453 (2002).

[30] J. B. Conrey, D. W. Farmer, and M. R. Zirnbauer, Howe pairs, supersymmetry, and ratios of random characteristic polynomials for the unitary groups u(n) (2007), arXiv:math-ph/0511024 [math-ph] .

[31] S. Pappalardi, L. Foini, and J. Kurchan, Physical Review Letters **129**, 170603 (2022).

[32] G. Cipolloni, L. Erdős, and D. Schröder, arXiv preprint arXiv:2102.09975 (2021).

[33] H. Ha, A. Morningstar, and D. A. Huse, Physical review letters **130**, 250405 (2023).

[34] J. Šuntajs and L. Vidmar, Physical Review Letters **129**, 060602 (2022).